The pinch technique at two-loops:
The case of mass-less Yang-Mills theories

Joannis Papavassiliou

Departamento de Física Teórica, Univ. Valencia
E-46100 Burjassot (Valencia), Spain

ABSTRACT

The generalization of the pinch technique beyond one loop is presented. It is shown that the crucial physical principles of gauge-invariance, unitarity, and gauge-fixing-parameter independence are instrumental for accomplishing this task, and is explained how the aforementioned requirements single out at two loops exactly the same algorithm which has been used to define the pinch technique at one loop, without any additional assumptions. The two-loop construction of the pinch technique gluon self-energy, and quark-gluon vertex are carried out in detail for the case of mass-less Yang-Mills theories, such as perturbative QCD. We present two different but complementary derivations. First we carry out the construction by directly rearranging two-loop diagrams. The analysis reveals that, quite interestingly, the well-known one-loop correspondence between the pinch technique and the background field method in the Feynman gauge *persists* also at two-loops. Since we use dimensional regularization the entire construction does not depend on the value of the space-time dimension d. The renormalization (when $d = 4$) is discussed in detail, and is shown to respect the aforementioned correspondence. Second, we present an absorptive derivation, exploiting the unitarity of the S-matrix and the underlying BRS symmetry; at this stage we deal only with tree-level and one-loop physical amplitudes. The gauge-invariant sub-amplitudes defined by means of this absorptive construction correspond precisely to the imaginary parts of the n-point functions defined in the full two-loop derivation, thus furnishing a highly non-trivial self-consistency check for the entire method. Various future applications are briefly discussed.

e-mail: Joannis.Papavassiliou@cern.ch;@uv.es

I. INTRODUCTION

The pinch technique (PT) was introduced by Cornwall [1], as the first step in the development of a self-consistent truncation scheme for the Schwinger-Dyson equations of QCD [2]. It was further developed in [3], and was generalized to theories with spontaneous symmetry breaking [4], and subsequently to the full Standard Model [5,6]. Various phenomenological applications were presented [7], and the one-loop correspondence between the PT and the background field method (BFM) [8–10] was established [11]. The important rôle of unitarity and analyticity was appreciated and exploited in a series of papers [12–15], which allowed the generalization of the Breit-Wigner formalism for unstable particles to the non-abelian sector of the Standard Model. Parallel developments took place in the field of finite temperature QCD [16], the concept of the QCD effective charge [2] was examined in detail [17], and subsequently applied to the field of renormalon calculus [18], and the generalized PT was presented [19]. In addition, a formalism for studying resonant CP violation [20] has been developed [21], and various issues related to the high-energy behaviour of the W-fusion process [22] have been resolved [23].

The PT reorganises systematically a given physical amplitude into sub-amplitudes, which have the same kinematic properties as conventional n-point functions, (propagators, vertices, boxes) [24], and are in addition endowed with important physical properties. The essential ingredient one uses in this rearrangement is the full exploitation of the elementary Ward identities (WI) of the theory, in order to enforce crucial cancellations. The various types of physical problems for which the PT can serve as a useful tool have been discussed frequently in the literature, most recently in [25] and [26].

So far the PT program has been carried out only at one-loop order, and its generalization to higher orders has been a long-standing question [27]. The general methodology of how the extension of the PT proceeds at two-loops has been presented in a recent brief communication [26]. There it was explained how the one-loop formalism, when properly interpreted and suitably adopted to the two-loop context, leads naturally to the PT extension. In this paper we will address the technical aspects of this procedure in detail, and will discuss extensively the plethora of physical issues involved.

We will present two independent constructions, which are however inextricably connected. The first one deals directly with the two-loop S-matrix element for the scattering process $q\bar{q} \rightarrow q\bar{q}$, exactly as was the case in the early one-loop PT applications. The first crucial ingredient is that of gauge-fixing parameter (GFP) independence. S-matrix elements are guaranteed to be GFP independent; in fact, as happens in the one-loop case, the cancellation of all GFP dependent terms proceeds by exploiting tree-level WI only, without having to carry out sub-integrations. This property is important, because it preserves the diagrammatic representation of the S-matrix, as well as the kinematic identity of the sub-amplitudes appearing in it (propagators,vertices,boxes). One can therefore, without loss of generality, choose a convenient gauge, such as the renormalizable Feynman gauge (RFG), provided that one considers the entire set of two-loop Feynman graphs contributing to the given S-matrix element

In the one-loop case the next step would be to split the bare three-gluon vertex appearing inside the one-loop quark-gluon vertex into a pinching and non-pinching contribution. This splitting is very special because it guarantees that the resulting effective Green's functions satisfy (at one-loop) naive, QED-like WI [2], instead of the usual Slavnov-Taylor identities [28]. As a consequence the effective one-loop gluon self-energy captures the running of the QCD coupling, exactly as happens with the photon vacuum polarization in QED. In the two-loop case the construction is lengthier but the crucial operation is precisely the same. One carries out the aforementioned splitting to all vertices whose one of the incoming momenta is the physical momentum transfer (or center-of-mass energy) of the process. As we will see in detail this splitting is sufficient to give rise to two-loop PT effective Green's functions which have the exact same properties as their one-loop counterparts.

The reason why all other three-gluon vertices inside the loops should remain unchanged (no splitting) can be understood by resorting to the special unitarity properties that the PT sub-amplitude must satisfy, a point which brings us to the second derivation. For this derivation we employ the unitarity and analyticity properties of the S-matrix, very much in the spirit presented in the more recent one-loop PT literature [13,14]. There, the precise diagrammatic correspondence between the one-loop (forward) process $q\bar{q} \rightarrow q\bar{q}$ and the tree-level process $q\bar{q} \rightarrow gg$ provided very useful, stringent constraints on the entire construction, rendering the method all the more powerful. These constraints are automatically encoded in the two-loop PT construction presented here; in fact they are even more constraining than in the previous order, for reasons that we will describe qualitatively now, and in great detail in the main body of the paper. The imaginary parts of the two-loop PT Green's functions are related by the optical theorem to precisely identifiable and very special parts of two different on-shell processes, the one-loop process $q\bar{q} \rightarrow gg$ and the tree-level process $q\bar{q} \rightarrow ggg$. In particular, the two-particle Cutkosky cuts of the two-loop PT self-energy

are related to the *PT rearranged s*-channel part of the one-loop $q\bar{q} \to gg$, while, at the same time, the three-particle Cutkosky cuts of the same quantity are related to the *PT rearranged s*-channel part of the tree-level $q\bar{q} \to ggg$; the latter is the *exact* analogue of the PT rearranged *s*-channel part of the tree-level $q\bar{q} \to gg$, already studied in the literature cited above.

The paper is organized as follows: In section II we present a brief overview of the one-loop PT algorithm, and discuss the most characteristic properties of the one-loop PT effective Green's functions. Here we follow the original PT formulation [2,3], and postpone the overview of the one-loop absorptive PT construction [13,14] until section V. In section III we present the full two-loop construction. This section contains three sub-sections, where we deal separately with the one-particle reducible graphs, the two-loop quark-gluon vertex, and the two-loop gluon self-energy. In the second sub-section we use at intermediate steps various results for the one-loop three-gluon vertex which are derived in section VI, and are more naturally integrated in the analysis presented there. Section III contains the main results of this paper; a major highlight is the proof that the correspondence between the PT and the Background Field Method Feynman gauge (BFMFG) persists at two-loops. In section IV we carry out the renormalization program in detail. We show that the two-loop PT Green's function can be renormalized by judiciously rearranging the existing counterterms, and that this procedure respects the correspondence between PT and BFMFG established in the previous section. In section V we present the general formalism and methodology of the absorptive PT construction; this second derivation is completely independent of the first, but at the same time is deeply connected to it. In this section we first derive various formulas which will be used in the next section, and present a thorough overview of the one-loop case. In section VI we present the two-loop absorptive derivation. There are two sub-sections: the first one contains a detailed discussion of the one-loop process $q\bar{q} \to gg$, and its rôle in enforcing the unitarity of the individual two-loop PT Green's functions; the second sub-section contains the study of the PT rearranged tree-level process $q\bar{q} \to ggg$, which demonstrates the crucial function of this process in realizing the aforementioned unitarity properties. Finally, in section VII we present our conclusions, and discuss possible connections with other work as well as future applications.

II. OVERVIEW OF THE ONE-LOOP CASE

In this section we briefly review the one-loop PT construction and establish some useful notation.

The fundamental tree-level three-gluon vertex $\Gamma^{(0)}_{\alpha\mu\nu}(q, p_1, p_2)$ is given by the following manifestly Bose-symmetric expression (all momenta are incoming, i.e. $q + p_1 + p_2 = 0$)

$$\Gamma^{(0)}_{\alpha\mu\nu}(q, p_1, p_2) = (q - p_1)_\nu g_{\alpha\mu} + (p_1 - p_2)_\alpha g_{\mu\nu} + (p_2 - q)_\mu g_{\alpha\nu} \,. \tag{2.1}$$

$\Gamma^{(0)}_{\alpha\mu\nu}(q, p_1, p_2)$ may be split into two parts [29]

$$\Gamma^{(0)}_{\alpha\mu\nu}(q, p_1, p_2) = \Gamma^{(0)}_{F\alpha\mu\nu}(q, p_1, p_2) + \Gamma^{(0)}_{P\alpha\mu\nu}(q, p_1, p_2) \,, \tag{2.2}$$

with

$$\Gamma^{(0)}_{F\alpha\mu\nu}(q, p_1, p_2) = (p_1 - p_2)_\alpha g_{\mu\nu} + 2q_\nu g_{\alpha\mu} - 2q_\mu g_{\alpha\nu} \,,$$
$$\Gamma^{(0)}_{P\alpha\mu\nu}(q, p_1, p_2) = p_{2\nu} g_{\alpha\mu} - p_{1\mu} g_{\alpha\nu} \,. \tag{2.3}$$

The vertex $\Gamma^{(0)}_{F\alpha\mu\nu}(q, p_1, p_2)$ is Bose-symmetric only with respect to the μ and ν legs. The first term in $\Gamma^{(0)}_{F\alpha\mu\nu}$ is a convective vertex describing the coupling of a gluon to a scalar field, whereas the other two terms originate from gluon spin or magnetic moment. $\Gamma^{(0)}_{F\alpha\mu\nu}(q, p_1, p_2)$ coincides with the BFMFG bare vertex involving one background (q) and two quantum (p_1, p_2) gluons [11]. Evidently the above decomposition assigns a special rôle to the q-leg, and allows $\Gamma^{(0)}_{F\alpha\mu\nu}$ to satisfy the Ward identity

$$q^\alpha \Gamma^{(0)}_{F\alpha\mu\nu}(q, p_1, p_2) = (p_2^2 - p_1^2) g_{\mu\nu} \,, \tag{2.4}$$

where the right hand-side (RHS) is the difference of two-inverse propagators in the FG, and vanishes "on shell", i.e. when $p_1^2 = p_2^2 = 0$. As has been explained in detail in [13,14], and as we will discuss extensively later on, the splitting of $\Gamma^{(0)}_{\alpha\mu\nu}(q, p_1, p_2)$ into $\Gamma^{(0)}_{F\alpha\mu\nu}(q, p_1, p_2)$ and $\Gamma^{(0)}_{P\alpha\mu\nu}(q, p_1, p_2)$ given in Eq. (2.2) has a natural interpretation in the context of the *tree-level* process $q(P)\bar{q}(P') \to g(p_1) + g(p_2)$ (annihilation channel), leading to an interesting connection with the optical theorem.

3

Consider next the S-matrix element for the quark (q)-antiquark $(\bar{q})$ elastic scattering process $q(P)\bar{q}(P') \to q(Q)\bar{q}(Q')$ in QCD; we set $q = P' - P = Q' - Q$, and $s = q^2$ is the square of the momentum transfer. One could equally well study the annihilation channel, in which case s would be the centre-of-mass energy. We will work in the RFG; this constitutes no loss of generality, as long as one studies the entire gauge-independent process. It is a straightforward but tedious exercise to convince one-self that through pinching, i.e. by simply exploiting the fundamental WI of Eq. (2.10), one can arrive at the set of diagrams of the RFG starting from the set of diagrams at any other value of ξ (see for example [30]), or even from the diagrams corresponding to non-covariant gauge-fixing schemes [31].

Let us define

$$t_{\mu\nu}(q) = q^2 g_{\mu\nu} - q_\mu q_\nu \,, \tag{2.5}$$

$$d(q) = \frac{-i}{q^2} \,, \tag{2.6}$$

$$S_0(p) = \frac{i}{\not{p} - m} \,, \tag{2.7}$$

$$\rho_{\mu\nu}(p) = \gamma_\mu S_0(p)\gamma_\nu \,. \tag{2.8}$$

$t_{\mu\nu}(q)$ is the *dimensionful* transverse tensor, and $S_0(p)$ is the tree-level quark propagator. In what follows we will use the short-hand notation $[dk] = \mu^{2\epsilon}\frac{d^d k}{(2\pi)^d}$ with $d = 4 - 2\epsilon$ the dimension of space-time and μ the 't Hooft mass. Furthermore we define the scalar quantities

$$J_1(q,k) = g^2 C_A[k^2(k+q)^2]^{-1} \,,$$
$$J_2(q,k) = g^2 C_A[k^4(k+q)^2]^{-1} \,,$$
$$J_3(q,\ell,k) = \frac{i}{2}g^2 C_A[k^2(k+\ell)^2(k+\ell-q)^2]^{-1} \,, \tag{2.9}$$

where C_A is the Casimir eigenvalue of the adjoint representation ($C_A = N$ for $SU(N)$). The quantities $J_2(q,k)$ and $J_3(q,\ell,k)$ will be used in later sections.

We then implement the vertex decomposition of Eq.(2.2) inside the non-Abelian one-loop quark-gluon vertex graph of Fig.1a, to be denoted by $\Gamma_\alpha^{(1),nab}(Q,Q')$, where now $p_{1\mu} = -k_\mu$, $p_{2\nu} = (k-q)_\nu$. The $\Gamma_{P\alpha\mu\nu}^{(0)}(q,p_1,p_2)$ term triggers the elementary Ward identity

$$\not{k} = (\not{k} + \not{Q} - m) - (\not{Q} - m) \,; \tag{2.10}$$

thus, a self-energy like piece is generated (Fig.1c), which is to be alloted to the conventional self-energy. In particular,

$$\Gamma_\alpha^{(1),nab}(Q,Q') = \widehat{\Gamma}_\alpha^{(1),nab}(Q,Q') + \frac{1}{2}V_{P\alpha\sigma}^{(1)}(q)\gamma^\sigma$$
$$+ X_{1\alpha}^{(1)}(Q,Q')(\not{Q}' - m) + (\not{Q} - m)X_{2\alpha}^{(1)}(Q,Q') \,, \tag{2.11}$$

where

$$\widehat{\Gamma}_\alpha^{(1),nab}(Q,Q') = \int [dk] J_1(q,k)\Gamma_{F\alpha\mu\nu}^{(0)}(q,-k,k-q)\rho^{\mu\nu}(Q') \,,$$

$$V_{P\alpha\sigma}^{(1)}(q) = 2\int [dk] J_1(q,k)\, g_{\alpha\sigma} \,,$$

$$X_{1\alpha}^{(1)}(Q,Q') = \int [dk] J_1(q,k)\gamma_\alpha S_0(Q') \,,$$

$$X_{2\alpha}^{(1)}(Q,Q') = \int [dk] J_1(q,k)S_0(Q')\gamma_\alpha \,. \tag{2.12}$$

The terms in the second line on the RHS of Eq.(2.11) vanish for on-shell external fermions. The (dimension-less) self-energy-like contribution $\frac{1}{2}V_{P\alpha\sigma}^{(1)}(q)$, together with another such contribution arising from the mirror vertex (not shown), after trivial manipulations gives rise to the dimensionful quantity

$$\Pi_{P\alpha\beta}^{(1)}(q) = V_{P\alpha\sigma}^{(1)}(q)t_\beta^\sigma(q) \,. \tag{2.13}$$

4

$\Pi_{P\alpha\beta}^{(1)}(q)$ will be added to the conventional one-loop two-point function $\Pi_{\alpha\beta}^{(1)}(q)$, to give rise to the the PT one-loop gluon self-energy $\widehat{\Pi}_{\alpha\beta}^{(1)}(q)$:

$$\widehat{\Pi}_{\alpha\beta}^{(1)}(q) = \Pi_{\alpha\beta}^{(1)}(q) + \Pi_{P\alpha\beta}^{(1)}(q)\,. \tag{2.14}$$

In particular, suppressing color indices throughout, we have that $\Pi_{\alpha\beta}^{(1)}(q)$ is given by the graphs of Fig 2a and Fig 2b, namely

$$\Pi_{\alpha\beta}^{(1)}(q) = \frac{1}{2} \int [dk] J_1(q,k) L_{\alpha\beta}(q,k)\,, \tag{2.15}$$

where

$$L_{\alpha\beta}(q,k) \equiv \Gamma_\alpha^{(0)\sigma\rho}(q,k,-k-q)\Gamma_{\beta\sigma\rho}^{(0)}(q,k,-k-q) - 2k_\alpha(k+q)_\beta\,, \tag{2.16}$$

and thus the PT one-loop gluon self-energy $\widehat{\Pi}_{\alpha\beta}^{(1)}(q)$ (Fig.2) assumes the closed form [3]

$$\widehat{\Pi}_{\alpha\beta}^{(1)}(q) = \frac{1}{2} \int [dk] J_1(q,k) \widehat{L}_{\alpha\beta}(q,k)\,, \tag{2.17}$$

with

$$\widehat{L}_{\alpha\beta}(q,k) \equiv \Gamma_{F\alpha}^{(0)\sigma\rho}(q,k,-k-q)\Gamma_{F\beta\sigma\rho}^{(0)}(q,k,-k-q) - 2(2k+q)_\alpha(2k+q)_\beta\,. \tag{2.18}$$

Notice that in general both $\Pi_{\alpha\beta}^{(1)}(q)$ and $\Pi_{P\alpha\beta}^{(1)}(q)$ on the RHS of Eq.(2.14) depend explicitly on the GFP in such a way as to give an GFP-independent sum.

In addition, gauge-invariance is encoded in the WI

$$q_\alpha \Pi_{\alpha\beta}^{(1)}(q) = q_\alpha \widehat{\Pi}_{\alpha\beta}^{(1)}(q) = 0\,. \tag{2.19}$$

The following important points have been discussed in detail in the literature (i) $\widehat{\Pi}_{\alpha\beta}(q)$ is independent of the gauge-fixing parameter in any gauge-fixing scheme. (ii) As happens in QED for the photon self-energy [32], the gluon self-energy $\widehat{\Pi}_{\alpha\beta}^{(1)}(q)$ captures the leading logarithms of the theory at that order [1,2] ; therefore the coefficient in front of the single logarithm coming from $\widehat{\Pi}_{\alpha\beta}^{(1)}(q)$, coincides with the first coefficient of the QCD β function [33]. (iii) $\widehat{\Pi}_{\alpha\beta}^{(1)}(q)$ can be Dyson resumed, following the diagrammatic algorithm presented in [12]. (iv) The combination $\alpha_{eff}(q,\mu) \sim g^2(\mu)\widehat{\Delta}(q/\mu)$, where $\widehat{\Delta}(q/\mu) = [1 - \widehat{\Pi}^{(1)}(q/\mu)]^{-1}$ is a renormalization-group-invariant quantity, and constitutes the non-abelian analogue of the QED concept of an effective charge [1,2,17]. Additional properties for the gluon two-point function have been presented in the literature for the case of non-abelian gauge theories with Higgs mechanism [4,6,12–15], and the (non-renormalizable) Kunimasa-Goto-Slavnov-Cornwall [34] massive Yang-Mills model [35].

The PT quark-gluon vertex $\widehat{\Gamma}_\alpha^{(1)}(Q,Q')$ is the sum of the non-abelian and abelian one-loop graphs, shown in Fig.3a and Fig.3b, which we will denote by $\widehat{\Gamma}_\alpha^{(1),nab}(Q,Q')$ and $\widehat{\Gamma}_\alpha^{(1),ab}(Q,Q')$, respectively. In addition to being GFP-independent, by virtue of Eq. (2.4) $\widehat{\Gamma}_\alpha^{(1)}(Q,Q')$ satisfies the following QED-like WI

$$q_\alpha \widehat{\Gamma}_\alpha^{(1)}(Q,Q') = \widehat{\Sigma}^{(1)}(Q) - \widehat{\Sigma}^{(1)}(Q'), \tag{2.20}$$

where $\widehat{\Sigma}^{(1)}$ is the PT one-loop quark self-energy, which coincides with the conventional one computed in the RFG. [30].

Finally, the PT one-loop n-point functions coincide with those computed in the BFMFG ("tilded" quantities) [11] , i.e.

$$\widehat{\Pi}_{\alpha\beta}^{(1)}(q) = \widetilde{\Pi}_{\alpha\beta}^{(1)}(q, \xi_Q = 1) \tag{2.21}$$

$$\widehat{\Gamma}_\alpha^{(1)}(Q,Q') = \widetilde{\Gamma}_\alpha^{(1)}(Q,Q',\xi_Q = 1) \tag{2.22}$$

$$\widehat{\Sigma}^{(1)}(Q) = \widetilde{\Sigma}^{(1)}(Q, \xi_Q = 1) = \Sigma^{(1)}(Q, \xi = 1) \tag{2.23}$$

In addition, exactly analogous properties have been established for the one-loop gluon three-point function [3] and four-point function ([36] and second paper in [11]).

III. THE FULL TWO-LOOP CONSTRUCTION

Here we present the full two-loop construction. The basic observation is the following: if one carries out the decomposition for the bare three-gluon vertex described in Eq. (2.2) to all *external* vertices (to be defined in sub-section IIIB) appearing in the Feynman diagrams contributing to the two-loop S-matrix element for the process $q\bar{q} \to q\bar{q}$, then two-loop sub-amplitudes will emerge, with precisely the same properties as the one-loop PT effective Green's functions.

Throughout this section we have used the following formulas, valid in dimensional regularization:

$$
\begin{aligned}
&\int \frac{[dk]}{k^2} = 0 \,, \\
&\int [dk] \frac{k_\alpha k_\beta}{k^4} = \left(\frac{1}{4 - 2\epsilon}\right) \int \frac{[dk]}{k^2} = 0 \,, \\
&\int [dk](2k + q)_\alpha J_1(q, k) = 0 \,, \\
&\int [dk] \frac{\ln^N(k^2)}{k^2} = 0 \quad N = 0, 1, 2, ...
\end{aligned}
\tag{3.1}
$$

The last relation guarantees the absence of tadpole and seagull contributions order by order in perturbation theory. In the two-loop calculation presented in this paper only the case $N = 1$ is relevant. Notice however that nowhere have we used the slightly subtler dimensional regularization result

$$
\int \frac{[dk]}{k^4} = 0 \,,
\tag{3.2}
$$

which is often employed in the literature. We also use the group theoretical identities

$$
\begin{aligned}
[\tau^a, \tau^b] &= i f^{abc} \tau^c \,, \\
f^{aex} f^{bex} &= C_A \delta^{ab} \,, \\
f^{axm} f^{bmn} f^{cnx} &= \frac{1}{2} C_A f^{abc} \,,
\end{aligned}
\tag{3.3}
$$

where τ^a are the gauge group generators in the fundamental representation; in the case of QCD $\tau^a = \lambda^a/2$, where λ^a are the Gell-Mann matrices.

The identity

$$
\begin{aligned}
\Gamma^{(0)}_{\alpha\mu\nu} \Gamma^{(0)\beta\mu\nu} &= \Gamma^{(0)}_{F\alpha\mu\nu} \Gamma^{(0)\beta\mu\nu}_F + \Gamma^{(0)}_{P\alpha\mu\nu} \Gamma^{(0)\beta\mu\nu}_F + \Gamma^{(0)}_{F\alpha\mu\nu} \Gamma^{(0)\beta\mu\nu}_P + \Gamma^{(0)}_{P\alpha\mu\nu} \Gamma^{(0)\beta\mu\nu}_P \\
&= \Gamma^{(0)}_{F\alpha\mu\nu} \Gamma^{(0)\beta\mu\nu}_F + \Gamma^{(0)}_{P\alpha\mu\nu} \Gamma^{(0)\beta\mu\nu} + \Gamma^{(0)}_{\alpha\mu\nu} \Gamma^{(0)\beta\mu\nu}_P - \Gamma^{(0)}_{P\alpha\mu\nu} \Gamma^{(0)\beta\mu\nu}_P
\end{aligned}
\tag{3.4}
$$

may also be found useful at intermediate steps.

The two-loop integration symbol

$$
(\mu^{2\epsilon})^2 \int \int \frac{d^d k}{(2\pi)^d} \frac{d^d \ell}{(2\pi)^d}
\tag{3.5}
$$

will be suppressed throughout. We define the following quantities

$$
\begin{aligned}
iI_1 &= g^4 C_A^2 [\ell^2 (\ell - q)^2 k^2 (k + \ell)^2 (k + \ell - q)^2]^{-1} \,, \\
iI_2 &= g^4 C_A^2 [\ell^2 (\ell - q)^2 k^2 (k + q)^2]^{-1} \,, \\
iI_3 &= g^4 C_A^2 [\ell^2 (\ell - q)^2 k^2 (k + \ell)^2]^{-1} \,, \\
iI_4 &= g^4 C_A^2 [\ell^2 \ell^2 (\ell - q)^2 k^2 (k + \ell)^2]^{-1} \,, \\
iI_5 &= g^4 C_A^2 [\ell^2 k^2 (k + q)^2]^{-1} \,,
\end{aligned}
\tag{3.6}
$$

which will be used extensively in what follows.

A. The one-particle reducible graphs

As has been explained in detail in [12] the resummability of the one-loop PT self-energy requires the conversion of one-particle reducible (1PR) strings of conventional self-energies $\Pi^{(1)}$ into strings containing PT self-energies $\widehat{\Pi}^{(1)}$. The process of converting conventional strings into PT strings gives rise to left-overs, which are effectively one-particle irreducible (1PI), and must be alloted to the genuine 1PI two-loop structures. Various self-consistency arguments supporting the validity of this method have been presented in the literature [37]; as we will see at the end of the third sub-section, the extension of the PT to two loops provides the ultimate test for the self-consistency of this procedure. It is straightforward to establish that the set of 1PI graphs (Fig.4a - Fig.4d) may be converted into the equivalent set of 1PI PT graphs (Fig.4e - Fig.4h), up to some missing pieces:

$$(4a) = (4e) - R^{(2)}_{P\,\alpha\beta}(q) \tag{3.7}$$

$$(4b) + (4c) + (4d) = (4f) + (4g) + (4h) - F^{(2)}_{P\,\alpha}(Q, Q') \tag{3.8}$$

with

$$iR^{(2)}_{P\,\alpha\beta}(q) = \Pi^{(1)}_{\alpha\rho}(q)V^{(1)\rho}_{P\beta}(q) + \frac{3}{4}\Pi^{(1)}_{P\,\alpha\rho}(q)V^{(1)\rho}_{P\,\beta}(q), \tag{3.9}$$

$$F^{(2)}_{P\,\alpha}(Q, Q') = \Pi^{(1)\beta}_{P\,\alpha}(q)d(q)\widehat{\Gamma}^{(1)}_{\beta}(Q, Q') + Y^{(2)}_{P\alpha}(Q, Q'), \tag{3.10}$$

with

$$Y^{(2)}_{P\alpha}(Q, Q') \equiv X^{(1)}_{1\alpha}(Q, Q')\Sigma^{(1)}(Q) + X^{(1)}_{2\alpha}(Q, Q')\Sigma^{(1)}(Q'). \tag{3.11}$$

The above terms originate from carrying out the vertex decomposition of Eq. (2.2) at all conventional 1PI diagrams. For example, the term $Y^{(2)}_{P\alpha}(Q, Q')$ (Fig 5b) originates after imposing Eq. (2.2) on the diagram of Fig.5a ; in addition, one obtains the PT counterpart of Fig.5a, namely Fig.5a^F, and the graph of Fig.5c, which is part of Fig.4f. The terms $R^{(2)}_{P\,\alpha\beta}(q)$ has been derived in detail in [12]. Notice that

$$R^{(2)}_{P\,\alpha\beta}(q) = I_2 \left[L_{\alpha\beta}(q, k) + 3t_{\alpha\beta}(q) \right]. \tag{3.12}$$

B. The two-loop vertex

In this sub-section we will demonstrate the construction of the two-loop PT quark-gluon vertex $\widehat{\Gamma}^{(2)}_{\alpha}(Q, Q')$, which turns out to have the exact same properties as its one-loop counterpart $\widehat{\Gamma}^{(1)}_{\alpha}(Q, Q')$. At the same time we will determine the two-loop propagator-like contributions $V^{(2)}_{P\alpha\sigma}\gamma_{\sigma}$, which will be subsequently converted into $\Pi^{(2)}_{P\alpha\sigma}$, i.e. the two-loop version of $\Pi^{(1)}_{P\alpha\sigma}$ of Eq.(2.13). In addition, out of this procedure the terms $Y^{(2)}_{P\alpha}(Q, Q')$ of Eq.(3.11) will emerge.

The construction proceeds as follows: The Feynman graphs contributing to $\Gamma^{(2)}_{\alpha}(Q, Q')$ can be classified into two sets. (a) those containing an "external" three-gluon vertex i.e. a three-gluon vertex where the momentum q is incoming, as shown Fig.6 and Fig.7, (b) those which do not have an "external" three-gluon vertex. This latter set contains either graphs with no three gluon vertices (abelian-like), or graphs with three-gluon vertices whose all three legs are irrigated by virtual momenta, i.e. q never enters alone into any of the legs; such would be for example the abelian graph of Fig.3b, if one was to insert a one-loop self-energy correction to the internal gluon line [38]). Of course, all three-gluon vertices appearing in the computation of the one-loop S-matrix are external, and so are those appearing in the 1PR part of the two-loop S-matrix (see previous section). Then one carries out the decomposition of Eq. (2.2) to the external three-gluon vertex of all graphs belonging to set (a), leaving *all* their other vertices unchanged, and identifies the propagator-like pieces generated at the end of this procedure.

The calculation is straightforward, but lengthy; it is more economical to identify the sub-structure of the one-loop three-gluon vertex $\Gamma^{(1)}_{\alpha\mu\nu}(q, p_1, p_2)$ (Fig K) nested inside the two-loop graph, Fig(Na1), and use the results presented in section VI, Eq. (6.35). To that end we must set $p_1 \to -\ell$ and $p_2 \to \ell - q$, and $J_3(q, -p_1, k) \to J_3(q, \ell, k)$, and rewrite the $\Gamma^{(1)}_{P\,\alpha\mu\nu}$ of Eq.(6.35) as follows

$$\Gamma^{(1)}_{P\,\alpha\mu\nu}(q,-\ell,\ell-q) = \left[J_3\left[\Gamma^{(0)}_{\nu\rho\alpha}(\ell-q,k,-k-\ell+q)+k_\nu g_{\alpha\rho}\right]\ell^\rho - \frac{i}{2}\,V^{(1)}_{P\alpha\nu}(q)\right]\ell_\mu$$

$$+\left[J_3\left[\Gamma^{(0)}_{\mu\alpha\rho}(-\ell,k+\ell,-k)+k_\mu g_{\alpha\rho}\right](\ell-q)^\rho - \frac{i}{2}\,V^{(1)}_{P\alpha\mu}(q)\right](\ell-q)_\nu$$

$$-\left[J_3\left[\Gamma^{(0)}_{\nu\mu\alpha}(\ell-q,k,-k-\ell+q)+k_\nu g_{\alpha\mu}\right]+\frac{1}{2}\,d(q)q_\alpha V^{(1)}_{P\mu\nu}(q)\right]\ell^2$$

$$-\left[J_3\left[\Gamma^{(0)}_{\mu\alpha\nu}(-\ell,k+\ell,-k)+k_\mu g_{\alpha\nu}\right]-\frac{1}{2}\,d(q)q_\alpha V^{(1)}_{P\mu\nu}(q)\right](\ell-q)^2$$

$$(3.13)$$

Thus we have (we omit the external spinors, and use $Q' = Q + q$)

$$(6a_1) = (6a_1^F) + \frac{1}{2}\Pi^{(1)\beta}_{P\alpha}(q)d(q)\Gamma^{(1),nab}_{\beta}(Q,Q')$$

$$+\frac{1}{2}\left[2I_2 g_{\alpha\sigma} - I_1[\Gamma^{(0)}_{\rho\sigma\alpha}(-k,-\ell,k+\ell)+k_\sigma g_{\alpha\rho}](\ell-q)^\rho\right]\gamma^\sigma$$

$$+D_1 + D_2 + D_3 + D_4 \tag{3.14}$$

$$(6b_1) = (6b_1^F) + \frac{1}{4}I_3 g_{\alpha\sigma}\gamma^\sigma - D_1 + D_5 + D_6 \tag{3.15}$$

$$(6b_1)' = (6b_1^F)' + \frac{1}{4}I_3 g_{\alpha\sigma}\gamma^\sigma - D_2 + D_7 + D_8 \tag{3.16}$$

$$(6c_1) = (6c_1^F) + \frac{1}{2}I_4 L_{\alpha\sigma}(\ell,k)\gamma^\sigma \tag{3.17}$$

$$(7r_i) = (7r_i^F) + \frac{1}{2}\Pi^{(1)\beta}_{P\alpha}(q)d(q)\Gamma^{(1),ab}_{\beta}(Q,Q') + \frac{1}{2}Y^{(2)}_{P\alpha}(Q,Q')$$

$$-(D_3 + D_4 + D_5 + D_6 + D_7 + D_8) \tag{3.18}$$

where

$$D_1 = -I_3[\Gamma^{(0)}_{\alpha\mu\nu}(\ell,k,-\ell-k)+k_\nu g_{\alpha\mu}]\{\gamma^\nu S(Q+\ell+k)\gamma^\mu\},$$

$$D_2 = I_3[\Gamma^{(0)}_{\alpha\nu\mu}(\ell,-\ell-k,k)+k_\mu g_{\alpha\nu}]\{\gamma^\nu S(Q'-\ell-k)\gamma^\mu\},$$

$$D_3 = -\frac{1}{2}I_5 q_\alpha\{\gamma_\mu S(Q+\ell)\gamma^\mu\},$$

$$D_4 = \frac{1}{2}I_5 q_\alpha\{\gamma_\mu S(Q'+\ell)\gamma^\mu\},$$

$$D_5 = -I_5\{\gamma_\alpha S(Q-k)\gamma_\mu S(Q-k-\ell)\gamma^\mu\},$$

$$D_6 = I_5\{\gamma_\alpha S(Q-k)\gamma_\mu S(Q+\ell)\gamma^\mu\},$$

$$D_7 = -I_5\{\gamma_\mu S(Q-k-\ell)\gamma^\mu S(Q-k)\gamma_\alpha\},$$

$$D_8 = I_5\{\gamma_\mu S(Q+\ell)\gamma^\mu S(Q-k)\gamma_\alpha\}, \tag{3.19}$$

Before we proceed the following comments are warranted:

(i) In the above formulas appropriate shiftings and relabellings of the integration momenta have been carried out, in order for the answer to be expressed in terms of the five basic denominators I_i defined in Eq.(3.6).

(ii) The topologies of D_1, D_2, D_3, D_4, D_5, and D_6 are shown in Fig.$6a_4$, Fig.$6a_5$, Fig.$6a_6$, Fig.$6a_7$, Fig.$6b_4$, and Fig.$6b_5$, respectively. $(6b_1)'$ corresponds to the figure obtained from Fig.$6b_1$ by drawing the internal three-gluon vertex on the other leg of the external three-gluon vertex, i.e. the leg which hooks onto the external spinor carrying momentum Q' (not shown); D_7 (shown in Fig.7h) and D_8 (not shown) are the analogues of D_5 and D_6 for the $(6b_1)'$ topology. Furthermore, the second and third term on the RHS of Eq.(3.14) are depicted in Fig.$6a_2$ and Fig.$6a_3$ respectively, the second term on the RHS of Eq.(3.15) is shown in Fig.$6b_2$, the second term on the RHS of Eq.(3.17) is shown in Fig.$6c_2$, and the second term on the RHS of Eq.(3.18) in Fig.$7c_a$.

(iii) The graph in Fig.$7r_2$ is accompanied by the graph with the abelian vertex correction on the other side (not shown). The graph containing the bare four-gluon vertex is not shown either.

(iv) Notice that the propagator-like part in Fig.7a is connected to the rest of the graph by a factor $g_{\alpha\beta}$; since this term will become part of the 1PR graph of Fig. 4c it must be supplemented a longitudinal component $q_\alpha q_\beta$. This contribution is proportional to the terms shown in Fig.7a_6 and Fig.7a_7 (remember that the latter are proportional to q_α), but notice that the color factors are different; the terms shown in Fig.6a_6 and Fig.6a_7 are proportional to C_A^2, whereas the term missing in Fig.(Sa) will have both C_A^2 and $C_A C_f$, where C_f is the Casimir for the τ_α representation of the (external) quarks. It is easy to show that these terms vanish when the external fermions are on shell, which is our case. In order to prove that one does not have to assume that q_α hits a conserved current on the other side of the graph; instead one notices that the terms in question are proportional to $[\Sigma^{(1)}(\mathcal{Q}, m) - \Sigma^{(1)}(\mathcal{Q}', m)]$, which vanishes when $\mathcal{Q} = \mathcal{Q}' = m$.

(v) Notice the appearance of propagator-like terms (Fig.6a_3, Fig.6b_2, and Fig.6c_2)

Adding Eq.(3.14) – Eq.(3.18), by parts, and using Eq.(3.11), we find

$$\Gamma_\alpha^{(2)}(Q, Q') = \frac{1}{2} F_{P\,\alpha}^{(2)}(Q, Q') + \frac{1}{2} V_{P\alpha\sigma}^{(2)} \gamma^\sigma + \widehat{\Gamma}_\alpha^{(2)}(Q, Q') \tag{3.20}$$

with

$$V_{P\alpha\sigma}^{(2)}(q) = I_4 L_{\alpha\sigma}(\ell, k) + (2I_2 + I_3) g_{\alpha\sigma} - I_1 \left[k_\sigma g_{\alpha\rho} + \Gamma_{\rho\sigma\alpha}^{(0)}(-k, -\ell, k+\ell) \right] (\ell - q)^\rho \tag{3.21}$$

The interpretation of the three terms appearing on the RHS of Eq.(3.20) is as follows:

(i) The term $\frac{1}{2} F_{P\,\alpha}^{(2)}(Q, Q')$ is half of the vertex-like part necessary to cancel the corresponding term appearing in Eq.(3.8), during the conversion of conventional 1PR graphs into their PT counterparts. The other half will come from the mirror vertex (not shown).

(ii) $\frac{1}{2} V_{P\alpha\sigma}^{(2)} \gamma^\sigma$ is the total propagator-like term originating from the two-loop quark-gluon vertex; together with the equal contribution from the mirror set of two-loop vertex graphs (not shown) will give rise to the self-energy term

$$\Pi_{P\alpha\beta}^{(2)}(q) = V_{P\alpha\sigma}^{(2)}(q) t_\beta^\sigma(q), \tag{3.22}$$

which will be part of the effective two-loop PT gluon self-energy, to be constructed in the next sub-section

(iii) $\widehat{\Gamma}_\alpha^{(2)}(Q, Q')$ is the PT two-loop quark-gluon vertex; it *coincides* with the corresponding two-loop quark-gluon vertex computed in the BFMFG, i.e.

$$\widehat{\Gamma}_\alpha^{(2)}(Q, Q') = \widetilde{\Gamma}_\alpha^{(2)}(Q, Q', \xi_Q = 1) \tag{3.23}$$

as happens in the one-loop case , Eq.(2.22). Either by virtue of the above equality and the formal properties of the BFM, or by means of an explicit diagrammatic calculation where one acts with q_α on individual diagrams, one can establish that $\widehat{\Gamma}_\alpha^{(2)}(Q, Q')$ satisfies the following QED-like WI

$$q_\alpha \widehat{\Gamma}_\alpha^{(2)}(Q, Q') = \widehat{\Sigma}^{(2)}(Q) - \widehat{\Sigma}^{(2)}(Q'), \tag{3.24}$$

which is the exact two-loop analogue of Eq.(2.20). $\widehat{\Sigma}^{(2)}(Q)$ is the two-loop PT fermion self-energy which satisfies

$$\widehat{\Sigma}^{(2)}(Q) = \widetilde{\Sigma}^{(2)}(Q, \xi_Q = 1) = \Sigma^{(2)}(Q, \xi = 1) \tag{3.25}$$

Again, this is the precise generalization of the one-loop result of Eq.(2.23). At this point this result comes as no surprise, since all three gluon vertices appearing in the Feynman graphs contributing to $\Sigma^{(2)}(Q, \xi)$ are internal; therefore, at $\xi = 1$ there will be no pinching [39].

We emphasize that the above result is non-trivial; indeed, even if one accepts that the appearance of the first and third term in Eq.(3.20), for example, could be forced, there is no a-priory reason why the remainder should turn out to be purely self-energy-like. Notice also that in deriving the above results no integrations (or sub-integrations) over virtual momenta have been carried out.

C. The two-loop self-energy

The construction of $\widehat{\Pi}_{\alpha\beta}^{(2)}(q)$ proceeds as follows: To the conventional two-loop gluon self-energy $\Pi_{\alpha\beta}^{(2)}(q)$ we add two additional terms; (i) the propagator-like term $\Pi_{P\alpha\beta}^{(2)}(q)$ derived in the previous sub-section, Eq.(3.22), and (ii) the

propagator-like part $-R_{P\,\alpha\beta}^{(2)}(q)$ given in Eq.(3.9), stemming from the conversion of the conventional string into a PT string; this term must be removed from the 1PR reducible set and be alloted to $\widehat{\Pi}_{\alpha\beta}^{(2)}(q)$, as described in [12]. Thus, $\widehat{\Pi}_{\alpha\beta}^{(2)}(q)$ reads

$$\widehat{\Pi}_{\alpha\beta}^{(2)}(q) = \Pi_{\alpha\beta}^{(2)}(q) + \Pi_{P\,\alpha\beta}^{(2)}(q) - R_{P\,\alpha\beta}^{(2)}(q)\,. \tag{3.26}$$

Up to minor notational modifications, this last equation is in fact identical to Eq.(3.5) in the second paper of [12], except that now we know the exact closed expression for the term $\Pi_{P\,\alpha\beta}^{(2)}(q)$.

It is a lengthy but relatively straightforward exercise to establish that in fact

$$\widehat{\Pi}_{\alpha\beta}^{(2)}(q) = \widetilde{\Pi}_{\alpha\beta}^{(2)}(q, \xi_Q = 1) \tag{3.27}$$

To see that in detail, we simply start out with the diagrams contributing to $\Pi_{\alpha\beta}^{(2)}(q)$ and convert them into the corresponding diagrams contributing to $\widetilde{\Pi}_{\alpha\beta}^{(2)}(q, \xi_Q = 1)$; in doing so we only need to carry out algebraic manipulations in the numerators of individual Feynman diagrams, and the judicious use of the identity of Eq.(3.4). The individual diagrams yield:

$$(8a) = (9a) + (9m) + (9n) + (9o) + (9p) + (9q) + (9r) + (9s)$$
$$+ I_1\left[\ell_\beta\ell^\rho k^\sigma \Gamma_{\alpha\sigma\rho}^{(0)}(q, k + \ell - q, -k - \ell) + (\ell \cdot q - \ell^2)(k + \ell - q)_\alpha (\frac{3}{2}\ell - q)_\beta\right]$$
$$+ I_1[k_\sigma g_{\alpha\rho} + \Gamma_{\rho\sigma\alpha}^{(0)}(-k, -\ell, k + \ell)](l - q)^\rho t_\beta^\sigma(q) - (2I_2 + I_3)t_{\alpha\beta}(q)$$
$$+ I_2\left[\frac{3}{8}t_{\alpha\beta}(q) + \frac{9}{16}q_\alpha q_\beta\right] - \frac{9}{2}I_3\left[\ell_\alpha(\ell - q)_\beta + (\ell \cdot q - \ell^2)g_{\alpha\beta}\right]$$
$$+ I_2[L_{\alpha\beta}(q, k) + 2k_\alpha(k + q)_\beta] - I_3[L_{\alpha\beta}(\ell, k) + 2k_\alpha(k + \ell)_\beta]$$
$$- I_3\left[3\ell_\alpha\ell_\beta - \frac{21}{8}q_\alpha\ell_\beta + q_\alpha q_\beta\right]$$

$$(8b) + (8c) = (9b) + (9c) + \frac{9}{2}I_3\left[\ell_\alpha(\ell - q)_\beta + (\ell \cdot q - \ell^2)g_{\alpha\beta}\right]$$

$$(8d) = (9d) + \frac{21}{8}I_2 t_{\alpha\beta}(q)$$

$$(8e) + (8f) = (9e) + (9f) - I_1\ell_\beta\ell^\rho k^\sigma\Gamma_{\alpha\sigma\rho}^{(0)}(q, k + \ell - q, -k - \ell)$$
$$- I_2\left[2k_\alpha(k + q)_\beta + \frac{1}{2}q_\alpha q_\beta\right] + I_3\left[2k_\alpha(k + \ell)_\beta + \frac{1}{4}q_\alpha\ell_\beta\right]$$

$$(8g) + (8h) = (9g) + (9h) + I_3 L_{\alpha\beta}(\ell, k) - I_4 L_{\alpha\sigma}(\ell, k)t_\sigma^\beta(q)$$

$$(8i) = (9i) - I_1\,(\ell \cdot q - \ell^2)(k + \ell - q)_\alpha(\frac{3}{2}\ell - q)_\beta - \frac{1}{16}I_2 q_\alpha q_\beta + \frac{1}{8}I_3 q_\alpha\ell_\beta$$

$$(8j) + (8k) = (9j) + (9k) + I_3[3\ell_\alpha\ell_\beta - 3\ell_\alpha q_\beta + q_\alpha q_\beta]$$

$$(8\ell) = (9\ell) \tag{3.28}$$

Adding the above equations by parts we find

$$\Pi_{\alpha\beta}^{(2)}(q) = \widetilde{\Pi}_{\alpha\beta}^{(2)}(q, \xi_Q = 1) + I_2\left[L_{\alpha\beta}(q, k) + 3t_{\alpha\beta}(q)\right] - I_4 L_{\alpha\sigma}(\ell, k)t_\sigma^\beta(q)$$

$$+ I_1\left[k_\sigma g_{\alpha\rho} + \Gamma_{\rho\sigma\alpha}^{(0)}(-k, -\ell, k + \ell)\right](l - q)^\rho t_\sigma^\beta(q) - (2I_2 + I_3)t_{\alpha\beta}(q)$$

$$\tag{3.29}$$

Using Eq.(3.21) and Eq.(3.12), Eq.(3.29) becomes

$$\Pi^{(2)}_{\alpha\beta}(q) = \widetilde{\Pi}^{(2)}_{\alpha\beta}(q, \xi_Q = 1) - \Pi^{(2)}_{P\,\alpha\beta}(q) + R^{(2)}_{P\,\alpha\beta}(q). \tag{3.30}$$

From Eq.(3.30) and Eq.(3.26) we arrive immediately to Eq.(3.27). Again, no integrations over virtual momenta need be carried out, except for identifying vanishing contributions by means of the formulas listed in Eq.(3.1).

Since we have used dimensional regularization throughout and no integrations have been performed the results of this section do not depend on the value d of the space-time; in particular they are valid for $d = 3$, which is of additional field-theoretical interest [40]. Clearly, when $d \to 4$ the renormalization program needs be carried out; this will be the subject of the next section.

IV. RENORMALIZATION

In this section we will carry out the renormalization for the two-loop PT Green's functions constructed in the previous section. There is of course no doubt that if one supplies the correct counterterms within the conventional formulation, the total S-matrix will continue being renormalized, even after the PT rearrangement of the (unrenormalized) two-loop Feynman graphs. The point of this section is to show a stronger version of renormalizability, i.e. that the new Green's function constructed through the PT rearrangement are *individually* renormalizable. The general methodology is as follows: We start out with the counterterms which are necessary to renormalize individually the conventional Green's functions contributing to the two-loop S-matrix. Then we will show that by simply rearranging them, following the PT rules, we will arrive at renormalized two-loop PT Green's functions.

We will use the following notation: Z_1 is the vertex renormalization constant for the conventional quark-gluon vertex Γ_α, Z_2 is the wave-function renormalization for the (external) quarks, Z_A the gluon wave-function renormalization corresponding to the conventional gluon self-energy Π, $\widehat{Z}_A$ the gluon wave-function renormalization corresponding to the PT gluon self-energy $\widehat{\Pi}$, Z_3 is the vertex renormalization constant for the conventional one-loop three-gluon vertex $\Gamma^{(1)}_{\alpha\mu\nu}$, and Z_{3F} the vertex renormalization constant for the $\Gamma^{(1)}_{F\,\alpha\mu\nu}$, $\bar{Z}_2$ is the ghost wave-function renormalization, and $\bar{Z}_1$ the ghost-gluon vertex renormalization constant. Equivalently, one can carry out the renormalization program using appropriately defined counter-terms. The corresponding counterterms, which, when added to the above n-loop quantities render them UV finite, are, respectively $K^{(n)}_1$, $K^{(n)}_2$, $K^{(n)}_A$, $\widehat{K}^{(n)}_A$, $K^{(n)}_3$, $K^{(n)}_{3F}$ $\bar{K}^{(n)}_2$, and $\bar{K}^{(n)}_1$. In addition, mass counterterms δm must be supplied if the quarks are considered to be massive. In a moment we will also introduce the counterterm $\widehat{K}^{(n)}_P$, which renders $V^{(n)}_P$ ultra-violet finite. Notice that because of the QED-like WI it satisfies $\widehat{\Gamma}_\mu$ becomes ultraviolet finite when the counterterm K_2 is added to it. The Zs and the Ks are related as follows :

$$Z_i = 1 + \sum_{j=1} K^{(j)}_i \quad i = 1, 2, 3$$

$$Z_A = 1 + \sum_{j=1} K^{(j)}_A$$

$$\widehat{Z}_A = 1 + \sum_{j=1} \widehat{K}^{(j)}_A$$

$$\bar{Z}_i = 1 + \sum_{j=1} \bar{K}^{(j)}_i \quad i = 1, 2$$

$$Z_g = 1 + \sum_{j=1} K^{(j)}_g$$

$$\delta m = \sum_{j=1} \delta m^{(j)} \tag{4.1}$$

We first begin with the 1PR part of the S-matrix. It is more convenient to work with dimension-less quantities; to that end we define the dimension-less gluon self-energy $\Pi^{(1)}$ simply through $\Pi^{(1)}_{\alpha\beta} = \Pi^{(1)} t_{\alpha\beta}$. In order to renormalize the extra pieces which must be alloted to the conventional 1PR graphs in order to convert them into their PT form, i.e. the $iR_P + F_P$ terms in Eq. (3.9) – Eq. (3.11), we must have (we use the superscript "R" to denote renormalizaed quantities)

$$iR^{(2)R}_P + F^{(2)R}_P = \Pi^{(1)R} V^{(1)R}_P + \frac{3}{4} V^{(1)R}_P V^{(1)R}_P + V^{(1)R}_P \widehat{\Gamma}^{(1)R} + Y^{(1)R}_P$$

$$= \frac{3}{4}(K^{(1)}_P + V^{(1)}_P)^2 + (\Pi^{(1)} - K^{(1)}_A)(V^{(1)}_P + K^{(1)}_P)$$

$$+(V_P^{(1)} + K_P^{(1)})(\widehat{\Gamma}^{(1)} + K_2^{(1)}) + (X_1^{(1)} + X_2^{(1)})\delta m^{(1)}$$
$$= iR_P^{(2)} + F_P^{(2)} + U_1^{(2)} + U_2^{(2)} \tag{4.2}$$

with

$$U_1^{(2)} = V_P^{(1)}\left[K_2^{(1)} - K_A^{(1)}\right] + K_P^{(1)}\left[\Pi^{(1)} + \Gamma^{(1)} + V_P^{(1)}\right] + (X_1^{(1)} + X_2^{(1)})\delta m^{(1)}$$

$$U_2^{(2)} = K_P^{(1)}\left[\frac{3}{4}K_P^{(1)} + K_2^{(1)} - K_A^{(1)}\right]. \tag{4.3}$$

Thus, the terms $U_1^{(2)}$ and $U_2^{(2)}$ need be supplied. Notice that the terms contained in $U_2^{(2)}$ are momentum independent (quadratic in the counterterms), whereas those contained in $U_1^{(2)}$ or momentum-dependent (linear in the counterterms). The latter will cancel against parts of the one-loop counterterms appearing inside the two-loop expressions for the conventional self-energy (Fig.10) and vertex (Fig.12), cancelling their sub-divergences. As for the former, they will become part of the final renormalization counterterm of the two-loop PT self-energy, i.e. the counterterm necessary for cancelling the remaining divergence, after the sub-divergences have been taken care of. Another way of saying this is that, since the extra terms R_P and F_P will be alloted to the PT gluon-self-energy and vertex, so should the counter-terms necessary to renormalize them.

We next show how the terms in $U_2^{(2)}$ are to be accounted for, and, at the same time, derive some useful relations among the various counterterms. The QED-like WI of equations Eq. (2.20) and Eq. (3.24) relating $\widehat{\Gamma}_\alpha^{(1)}$ and $\widehat{\Sigma}^{(1)}$, and $\widehat{\Gamma}_\alpha^{(2)}$ and $\widehat{\Sigma}^{(2)}$, respectively, imposes the following QED-like relation between the renormalization constants $\widehat{Z}_1$ and $\widehat{Z}_2$, up to order g^4:

$$\widehat{Z}_1 = \widehat{Z}_2. \tag{4.4}$$

In addition, from the WI of Eq. (6.36), we have to order g^2 (at least)

$$Z_{3F} = Z_A. \tag{4.5}$$

Notice also that Eq. (6.36) dictates that the ultraviolet-divergent part of $\Gamma_{F\,\alpha\mu\nu}^{(1)}$ is proportional to $\Gamma_{F\,\alpha\mu\nu}^{(0)}$ rather than $\Gamma_{F\,\alpha\mu\nu}^{(0)}$; had it been the other way around there would be no longitudinal ultraviolet-divergent pieces on the RHS of Eq. (6.36). As we will see, this "mismatch" will generate the pieces which in the BFM language give rise to the gauge-fixing renormalization of the vertices (Fig.10a and Fig.10b)

Furthermore, the renormalization constants before and after the PT rearrangements are related to the gauge coupling renormalization as follows:

$$Z_g^2 = Z_1^2 Z_2^{-2} Z_A^{-1}$$
$$= \widehat{Z}_1^2 \widehat{Z}_2^{-2} \widehat{Z}_A^{-1}$$
$$= \widehat{Z}_A^{-1}, \tag{4.6}$$

where Eq. (4.4) has been used. After substituting the expressions given in Eq. (4.1) into Eq. (4.6) and equating powers of the coupling constant g we arrive at the following relations for the corresponding counterterms

$$\widehat{K}_A^{(1)} = K_A^{(1)} - 2(K_1^{(1)} - K_2^{(1)}), \tag{4.7}$$
$$\widehat{K}_A^{(2)} = K_A^{(2)} - 2(K_1^{(2)} - K_2^{(2)}) + K_1^{(1)}[3K_1^{(1)} - 4K_2^{(1)} - 2K_A^{(1)}] + K_2^{(1)}[2K_A^{(1)} + K_2^{(1)}]. \tag{4.8}$$

Substituting the relations

$$K_1^{(j)} = \frac{1}{2}K_P^{(j)} + K_2^{(j)}, \qquad j = 1, 2 \tag{4.9}$$

into the above equations we obtain

$$\widehat{K}_A^{(1)} = K_A^{(1)} - K_P^{(1)}, \tag{4.10}$$
$$\widehat{K}_A^{(2)} = K_A^{(2)} - K_P^{(2)} + U_2^{(2)}, \tag{4.11}$$
$$\widehat{K}_A^{(1)} = -2K_g^{(1)}. \tag{4.12}$$

Notice that if $Z_1 = Z_2$, or equivalently, $K_P^{(j)} = 0$, then $Z_A = \widehat{Z}_A$, which is simply the QED case.

It is now clear what the rôle of the $U_2^{(2)}$ terms is; they must be added to the conventional two-loop self-energy counterterm $K_A^{(2)}$ and the part of the vertex counterterm corresponding to $V_P^{(2)}$; these two counterterms are already present, whereas the term $U_2^{(2)}$ must be borrowed from some other part of the S-matrix, in order for the initial equation Eq. (4.6) to be enforced.

We next turn to the $U_1^{(2)}$ terms. We will show that they will cancel precisely against terms originating from the rearrangement of the graphs shown in Fig.10 and Fig.12, in order to convert them into the graphs shown in Fig.11 and Fig.13. The former set contains the counterterms necessary for cancelling the one-loop sub-divergences inside the conventional two-loop gluon self-energy and quark-gluon vertex, the latter the counterterms needed for the two-loop PT gluon self-energy and quark-gluon vertex.

We begin with two-loop gluon self-energy shown in Fig.10. From the Slavnov-Taylor identity [28] we have that [41,42]

$$\frac{Z_3}{Z_A} = \frac{\bar{Z}_1}{\bar{Z}_2}\,, \tag{4.13}$$

from which we obtain [43]

$$K_3^{(1)} - K_A^{(1)} = \bar{K}_1^{(1)} - \bar{K}_2^{(1)} = \frac{1}{2}K_P^{(1)}\,. \tag{4.14}$$

This relation is important for what follows.

Then we have for the graphs of Fig.10:

$$(10a) + (10b) = K_3^{(1)} \int [dk] J_1(q,k) \Gamma_{\alpha\mu\nu}^{(0)} \Gamma_{\beta\mu\nu}^{(0)}$$
$$(10c) = (10c_1) + (10c_2)$$
$$(10d) + (10e) = \bar{K}_1^{(1)} \int [dk] J_1(q,k) k_\alpha (k+q)_\beta$$
$$(10f) + (10g) = -\bar{K}_2^{(1)} \int [dk] J_1(q,k) k_\alpha (k+q)_\beta \tag{4.15}$$

with

$$(10c_1) = -K_A^{(1)} \int [dk] J_1(q,k) \Gamma_{\alpha\mu\nu}^{(0)} \Gamma_{\beta\mu\nu}^{(0)}$$
$$(10c_2) = K_A^{(1)} \int [dk] J_2(q,k) k_\mu k_\sigma \Gamma_{\alpha\mu\nu}^{(0)} \Gamma_{\beta\sigma\nu}^{(0)}\,; \tag{4.16}$$

J_2 has been defined in Eq. (2.9). Thus, using Eq. (4.14) and Eq. (2.15) we obtain

$$[(10a) + (10b) + (10c_1)] + [(10d) + (10f)] + [(10e) + (10g)] = K_P^{(1)} \Pi_{\alpha\beta}^{(1)}(q) \tag{4.17}$$

Next, we write $(10c_2)$ as follows

$$(10c_2) = (11a) + (11b) + (11c) - 2t_{\alpha\sigma}(q) \int [dk] J_2(q,k) k_\beta k^\sigma \tag{4.18}$$

where

$$(11a) + (11b) = K_A^{(1)} \int [dk] J_1(q,k) \Gamma_{P\alpha\mu\nu}^{(0)} \Gamma_{F\beta}^{(0)\mu\nu}$$
$$(11c) = K_A^{(1)} \int [dk] J_2(q,k) k^\mu k_\sigma \Gamma_{F\alpha\mu\nu}^{(0)} \Gamma_{F\beta}^{(0)\sigma\nu} \tag{4.19}$$

We next convert the renormalization constants for the conventional two-loop quark-gluon vertex $\Gamma_\alpha^{(2)}$ (Fig.12) into those necessary for the PT 2-loop quark-gluon vertex $\widehat{\Gamma}_\alpha^{(2)}$ finite (Fig.13). We have:

13

$$(12a) = K_3^{(1)}\Gamma^{(1)} = (K_{3F}^{(1)} + \frac{1}{2}K_P^{(1)})\Gamma^{(1)} = (13a) + \frac{1}{2}K_P^{(1)}\Gamma^{(1)}$$

$$(12c) + (12d) = K_1^{(1)}V_P^{(1)} + (13c) + (13d)$$

$$(12e) = -\frac{1}{2}K_2^{(1)}V_P^{(1)} + \frac{1}{2}(X_1^{(1)} + X_2^{(1)})\delta m^{(1)} + (13e)$$

$$(12b) = -K_A^{(1)}\int [dk]J_2(q,k)\Gamma_{\alpha\sigma\nu}^{(0)}t_\mu^\sigma(k)\rho^{\mu\nu}(Q+k)$$

$$= -K_A^{(1)}\int [dk]J_2(q,k)(\Gamma_{F\alpha\sigma\nu}^{(0)} + \Gamma_{P\alpha\sigma\nu}^{(0)})t_\mu^\sigma(k)\rho^{\mu\nu}(Q+k)$$

$$= (13b) - K_A^{(1)}\int [dk]J_2(q,k)t_{\alpha\mu}(k)\gamma^\mu$$

$$= (13b) - \frac{1}{2}K_A^{(1)}V_P^{(1)} + K_A^{(1)}t_{\alpha\sigma}(q)\int [dk]J_2(q,k)k_\beta k^\sigma\gamma^\beta$$

$$(4.20)$$

Notice that the last term on the RHS of Eq. (4.20), together with an equal term from the mirror vertex graphs (not shown) will cancel against the last term in Eq.(4.18). Using that $K_1^{(1)} - \frac{1}{2}K_2^{(1)} = \frac{1}{2}(K_P^{(1)} + K_2^{(1)})$ we finally arrive at

$$K_{(Fig.10)} + 2K_{(Fig.12)} = K_{(Fig.11)} + 2K_{(Fig.13)} + U_1^{(1)} \qquad (4.21)$$

where the factors of 2 multiplying $K_{(Fig.12)}$ and $K_{(Fig.13)}$ account for the mirror vertex contributions. Evidently, the PT rearrangement gives rise to a term $U_1^{(1)}$, as announced.

The counterterms resulting from the above rearrangement are exactly those required to cancel all sub-divergences inside $\widehat{\Gamma}_\alpha^{(2)}(Q,Q')$; the latter coincide of course with the sub-divergences inside $\widetilde{\Gamma}_\alpha^{(2)}(Q,Q',\xi_Q = 1)$. To demonstrate that the counterterms shown in Fig.13 are in fact identical to those obtained when carrying out the BFM renormalization program as explained in [9], i.e. renormalizing only the background gluons, the external quarks, the coupling constant g, and the GFP (ξ_Q), one may proceed as follows: (i) start with graph (13b), and separate the $t_{\sigma\mu}(k)$ into the part proportional to $g_{\sigma\mu}$ and the part proportional to $k_\sigma k_\mu$; the second part is simply the gauge-fixing renormalization to the self-energy, as explained in [9]. (ii) Half of the piece proportional to $g_{\sigma\mu}$ must be added to (13a); the latter is proportional to $\Gamma^{(0)}$. Using that $K_{3F}^{(1)} = K_A^{(1)}$ (from Eq. (4.5)), the total contribution is proportional to $K_A^{(1)}(\Gamma^{(0)} - \Gamma_F^{(0)}) = K_A^{(1)}\Gamma_P^{(0)}$, which is the contribution from the gauge-fixing renormalization of the elementary BFM three-gluon vertex. (iii) The remaining half proportional to $g_{\sigma\mu}$ from step (i) must be split equally between $(13c) + \frac{1}{2}(13e)$ and $(13d) + \frac{1}{2}(13e)$. Each of these two combinations will then give a contribution proportional to $K_1^{(1)} - \frac{1}{2}K_2^{(1)} - \frac{1}{2}K_A^{(1)} = -\frac{1}{2}\widehat{K}_A^{(1)} + \frac{1}{2}K_2^{(1)} = K_g^{(1)} + \frac{1}{2}K_2^{(1)}$, where Eq. (4.9), Eq. (4.10), and Eq. (4.12) have been used in the last steps. The wave-function renormalization for the external fermions will then cancel $\frac{1}{2}K_2^{(1)}$, and $K_g^{(1)}$ will be re-absorbed into the gauge-coupling renormalization.

Notice that the correspondence between the PT and the BFMFG Green's functions established in the previous section persists after renormalization; the resulting expressions are the BFMFG renormalized quantities, as derived in [9]. An immediate consequence of this [9] is that the coefficient multiplying the logarithm of the PT two-loop self-energy is equal the the two-loop coefficient of the QCD β function [41,42], i.e. $(34/3)\,C_A^2$. It is also interesting to see how the PT rearrangement leads into the interpretation of counterterms generated from the QCD Lagrangian in the renormalized Feynman-gauge [42], as GFP renormalizations of the BFM Lagrangian [9].

V. THE ABSORPTIVE CONSTRUCTION: GENERAL FORMALISM

In the next two sections we will show in detail how one may construct the two-loop PT effective Green's functions using unitarity and analyticity arguments. This derivation generalizes the method first presented in [13] and [14] for the one-loop case, and constitutes a non-trivial self-consistency check for the entire approach. In this section we will set up the formalism, and discuss in detail the one-loop case, which will serve as the general paradigm for the two-loop generalization, to be presented in the following section. Apart from some minor modifications, in the next two sections we will adopt the notation used in [13].

The optical theorem for the case of forward scattering assumes the form

$$\Im m\langle a|T|a\rangle = \frac{1}{2}\sum_i (2\pi)^4 \delta^{(4)}(p_a - p_i)\langle i|T|a\rangle^* \langle i|T|a\rangle\,, \tag{5.1}$$

where the sum $\sum_i$ should be understood to be over the entire phase space of all allowed on-shell intermediate states i. After expanding the T matrix in powers of g, i.e. $T = \sum_{n=2} T^{[n]}$, we have that

$$\Im m\langle a|T^{[n]}|a\rangle = \frac{1}{2}\sum_i (2\pi)^4 \delta^{(4)}(p_a - p_i)\sum_k \langle i|T^{[k]}|a\rangle^* \langle i|T^{[n-k]}|a\rangle\,. \tag{5.2}$$

In particular, if in the initial states we have a q-$\bar{q}$ pair, i.e. $|a\rangle = |q\bar{q}\rangle$ we have for the first non-trivial orders, $n = 4$ and $n = 6$

$$\Im m\langle q\bar{q}|T^{[4]}|q\bar{q}\rangle = \frac{1}{2}\left(\frac{1}{2!}\right)\int (dPS)_{2g}\langle 2g|T^{[2]}|q\bar{q}\rangle^* \langle 2g|T^{[2]}|q\bar{q}\rangle\,, \tag{5.3}$$

and

$$\Im m\langle q\bar{q}|T^{[6]}|q\bar{q}\rangle = \frac{1}{2}\left(\frac{1}{3!}\right)\int (dPS)_{3g}\langle 3g|T^{[2]}|q\bar{q}\rangle^* \langle 3g|T^{[2]}|q\bar{q}\rangle$$
$$+ \frac{1}{2}\left(\frac{1}{2!}\right)\int (dPS)_{2g}2\Re e\left(\langle 2g|T^{[4]}|q\bar{q}\rangle^* \langle 2g|T^{[2]}|q\bar{q}\rangle\right)\,, \tag{5.4}$$

respectively [44]. $(dPS)_{2g}$ and $(dPS)_{3g}$ stand for the two- and three-body phase space for mass-less gluons, respectively. Next we introduce the short-hand notation

$$\mathcal{A}^{[n]} \equiv \Im m\langle q\bar{q}|T^{[n]}|q\bar{q}\rangle\,,$$
$$\mathcal{T}_m^{[k]} \equiv \langle mg|T^{[k]}|q\bar{q}\rangle \qquad m,k = 2,3,... \tag{5.5}$$

Then, Eq. (5.3) and Eq. (5.4) become respectively

$$\mathcal{A}^{[4]} = \frac{1}{2}\left(\frac{1}{2!}\right)\int (dPS)_{2g}\mathcal{T}_2^{[2]*}\mathcal{T}_2^{[2]}\,, \tag{5.6}$$

$$\mathcal{A}^{[6]} = \frac{1}{2}\left(\frac{1}{3!}\right)\int (dPS)_{3g}\mathcal{T}_3^{[3]*}\mathcal{T}_3^{[3]} + \frac{1}{2}\left(\frac{1}{2!}\right)\int (dPS)_{2g}2\Re e\left(\mathcal{T}_2^{[4]*}\mathcal{T}_2^{[2]}\right)$$
$$= \mathcal{A}_3^{[6]} + \mathcal{A}_2^{[6]}\,. \tag{5.7}$$

The quantities defined above have the explicit form

$$\mathcal{A}^{[4]} = \frac{1}{2}\left(\frac{1}{2!}\right)[\mathcal{T}_{2s}^{[2]} + \mathcal{T}_{2t}^{[2]}]_{\mu\nu}^{ab}P^{\mu\mu'}(p_1)P^{\nu\nu'}(p_2)[\mathcal{T}_{2s}^{[2]} + \mathcal{T}_{2t}^{[2]}]_{\mu'\nu'}^{ab*}\,, \tag{5.8}$$

$$\mathcal{A}_3^{[6]} = \frac{1}{2}\left(\frac{1}{3!}\right)[\mathcal{T}_{3s}^{[3]} + \mathcal{T}_{3t}^{[3]}]_{\mu\nu\rho}^{abc}P^{\mu\mu'}(p_1)P^{\nu\nu'}(p_2)P^{\rho\rho'}(p_3)[\mathcal{T}_{3s}^{[3]} + \mathcal{T}_{3t}^{[3]}]_{\mu'\nu'\rho'}^{abc*}\,, \tag{5.9}$$

$$\mathcal{A}_2^{[6]} = \left(\frac{1}{2!}\right)\Re e\left([\mathcal{T}_{2s}^{[4]} + \mathcal{T}_{2t}^{[4]}]_{\mu\nu}^{ab}P^{\mu\mu'}(p_1)P^{\nu\nu'}(p_2)[\mathcal{T}_{2s}^{[4]} + \mathcal{T}_{2t}^{[4]}]_{\mu'\nu'}^{ab*}\right)\,, \tag{5.10}$$

where we have suppressed the phase space integrations. $P_{\mu\nu}$ is the polarization tensor for mass-less gluons,

$$P_{\mu\nu}(p,n,\eta) = -g_{\mu\nu} + \frac{n_\mu p_\nu + n_\nu p_\mu}{np} - \eta\frac{p_\mu p_\nu}{(np)^2}\,, \tag{5.11}$$

with n_μ is an arbitrary four-vector, and η a gauge parameter.

15

We will now study the process $q(k_1)\bar{q}(k_2) \rightarrow g(p_1)g(p_2)$ at tree-level, using the equations derived above. This study will further elucidate the rôle of the Eq. (2.2) in enforcing perturbative unitarity at the level of individual Green's functions, and will set up the stage for the two-loop generalization.

The BRS symmetry [45] of the original Lagrangian leads to the following identities [46]:

$$p_1^\mu \mathcal{T}_{2\mu\nu}^{ab} = (S_2^{\{12\}})^{ab} p_{2\nu} \,,$$
$$p_2^\nu \mathcal{T}_{2\mu\nu}^{ab} = (S_2^{\{21\}})^{ab} p_{1\mu} \,,$$
$$p_2^\nu p_1^\mu \mathcal{T}_{2\mu\nu}^{ab} = 0 \,. \tag{5.12}$$

If we split the amplitude into an s-channel and t-channel contribution ($s = q^2 = (k_1 + k_2)^2 = (p_1 + p_2)^2$, and $t = (k_1 - p_1)^2 = (k_2 - p_2)^2$), the first of the identities in Eq. (5.12) becomes

$$p_1^\mu \left(\mathcal{T}_{2s} + \mathcal{T}_{2t} \right)_{\mu\nu}^{ab} = \left(S_{2s}^{\{12\}} + S_{2t}^{\{12\}} \right)^{ab} p_{2\nu} \,. \tag{5.13}$$

The remaining two identities are exactly analogous and will be suppressed throughout.

The PT rearrangement of the amplitude amounts to a special choice for $\mathcal{T}_{2s}$ and $\mathcal{T}_{2t}$, which will be denoted by $\mathcal{T}_{2s}^F$ and $\mathcal{T}_{2t}^F$, respectively. After defining these "Feynman" amplitudes, Eq. (5.13) reads

$$p_1^\mu \left(\mathcal{T}_{2s}^F + \mathcal{T}_{2t}^F \right)_{\mu\nu}^{ab} = \left(S_{2s}^{F\{12\}} + S_{2t}^{F\{12\}} \right)^{ab} p_{2\nu} \,, \tag{5.14}$$

and to order k,

$$p_1^\mu \left(\mathcal{T}_{2s}^{[k]F} + \mathcal{T}_{2t}^{[k]F} \right)_{\mu\nu}^{ab} = \left(S_{2s}^{[k]F\{12\}} + S_{2t}^{[k]F\{12\}} \right)^{ab} p_{2\nu} \,. \tag{5.15}$$

We will next study the case $k = 2$ (tree-level, Fig.14).

For "on-shell" gluons, i.e. $p^2 = 0$, $P_{\mu\nu}(p, n, \eta)$ of Eq. (5.11) satisfies the transversality condition $p^\mu P_{\mu\nu} = 0$. Thus one may immediately eliminate the $\Gamma_{P\alpha\mu\nu}^{(0)}(q, p_1, p_2)$ part of $\Gamma_{\alpha\mu\nu}^{(0)}(q, p_1, p_2)$, which vanishes when contracted with the term $P_{\mu\mu'}(p_1) P_{\nu\nu'}(p_2)$, and effectively replace $\Gamma_{\alpha\mu\nu}^{(0)}(q, p_1, p_2)$ by $\Gamma_{F\alpha\mu\nu}^{(0)}(q, p_1, p_2)$, as in Fig.14a. One then proceeds by recognizing that the longitudinal parts of the $P_{\mu\mu'}(p_1)$ and $P_{\nu\nu'}(p_2)$ trigger a fundamental cancellation [13,14] involving the s- and t- channel graphs (Fig.14a and Fig.14d), which is a consequence of the underlying BRS symmetry. In particular, the action of p_1^μ or p_2^ν on $\Gamma_{F\alpha\mu\nu}^{(0)}$ gives

$$p_1^\mu \Gamma_{F\alpha\mu\nu}^{(0)}(q, p_1, p_2) = (p_2 - p_1)_\alpha p_{2\nu} + (p_1^2 - p_2^2)g_{\alpha\nu} + t_{\alpha\nu}(q)$$
$$p_2^\nu \Gamma_{F\alpha\mu\nu}^{(0)}(q, p_1, p_2) = (p_2 - p_1)_\alpha p_{1\mu} + (p_1^2 - p_2^2)g_{\alpha\mu} - t_{\alpha\mu}(q) \tag{5.16}$$

The first term on the RHS of either equation cancels against an analogous contribution from the t-channel graph, whereas the second terms vanish for on-shell gluons. Finally, the terms proportional to $p_{2\nu}$ and $p_{1\mu}$ (Fig.14b) are such that all dependence on the unphysical four-vector n_μ and the parameter η vanishes, as it should. In addition, a residual (s-dependent) contribution emerges from these latter terms, which must be added to the parts stemming from the $g_{\mu\mu'}g_{\nu\nu'}$ part of the calculation. In particular [13], we have that

$$(\mathcal{T}_{2s}^F)_{\mu\nu}^{ab} = g\{\gamma_\alpha^m\}f^{mab}d(q)\Gamma_{F\mu\nu}^{(0)\alpha}(q, p_1, p_2) \,,$$
$$\mathcal{T}_{2t}^{[2]F} = \mathcal{T}_{2t}^{[2]} \,,$$
$$S_{2t}^{[2]F\{12\}} = S_{2t}^{[2]\{12\}} = 0 \,,$$
$$p_1^\mu (\mathcal{T}_{2s}^{[2]F})_{\mu\nu}^{ab} = (S_{2s}^{[2]F\{12\}})^{ab} p_{2\nu} + (\Lambda_2^{[2]F})_\nu^{ab} \,,$$
$$p_1^\mu (\mathcal{T}_{2t}^{[2]F})_{\mu\nu}^{ab} = -(\Lambda_2^{[2]F})_\nu^{ab} \,, \tag{5.17}$$

with

$$(\Lambda_2^{[2]F})_\nu^{ab} = g\{\gamma_\alpha^e\}f^{eab}d(q)t_\nu^\alpha(q)$$

$$\left(S_{2s}^{[2]F\{12\}}\right)^{ab} = g\{\gamma_\alpha^e\}f^{eab}d(q)(p_2 - p_1)^\alpha\,, \tag{5.18}$$

and $\{\gamma_\alpha^a\} = ig\bar{v}(k_2)\tau^a\gamma_\alpha u(k_1)$.

From the above results follows

$$p_1^\mu\left(\mathcal{T}_{2s}^{[2]F} + \mathcal{T}_{2s}^{[2]}\right)_{\mu\nu}^{ab} = \left(S_{2s}^{[2]F\{12\}}\right)^{ab}p_{2\nu}\,, \tag{5.19}$$

and thus

$$\mathcal{A}^{[4]} = \frac{1}{2}\left(\frac{1}{2!}\right)\left[\left(\mathcal{T}_{2s}^{[2]F} + \mathcal{T}_{2t}^{[2]}\right)\left(\mathcal{T}_{2s}^{[2]F} + \mathcal{T}_{2t}^{[2]}\right)^* - 2\left(S_{2s}^{[2]F\{12\}}\right)\left(S_{2s}^{[2]F\{12\}}\right)^*\right]$$

$$= \mathcal{A}_S^{[4]} + \mathcal{A}_V^{[4]} + \mathcal{A}_B^{[4]}\,, \tag{5.20}$$

with

$$\mathcal{A}_S^{[4]} = \frac{1}{2}\left(\frac{1}{2!}\right)\left[\mathcal{T}_{2s}^{[2]F}\mathcal{T}_{2s}^{[2]F*} - 2\left(S_{2s}^{[2]F\{12\}}\right)\left(S_{2s}^{[2]F\{12\}}\right)^*\right]\,,$$

$$\mathcal{A}_V^{[4]} = \frac{1}{2}\left(\frac{1}{2!}\right)\left[\mathcal{T}_{2s}^{[2]F}\mathcal{T}_{2t}^{[2]*} + \mathcal{T}_{2t}^{[2]}\mathcal{T}_{2s}^{[2]F*}\right]\,,$$

$$\mathcal{A}_B^{[4]} = \frac{1}{2}\left(\frac{1}{2!}\right)\mathcal{T}_{2t}^{[2]}\mathcal{T}_{2t}^{[2]*}\,. \tag{5.21}$$

In the last step we have defined self-energy (S), vertex (V) and box (B) -like amplitudes, according to their dependence on the Mandelstam variables s and t as in the case of a scalar filed theory, or QED; $\mathcal{A}_S^{[4]}$ depends only on s, $\mathcal{A}_V^{[4]}$ on s and t, and $\mathcal{A}_B^{[4]}$ only on t.

The next step is to identify these sub-amplitudes as the imaginary parts of the effective one-loop self-energy, vertex, and box, under construction. For example, for the effective self-energy $\widehat{\Pi}^{\alpha\beta}(q)$ we will proceed as follows: first write $\mathcal{A}_S^{[4]}$ in the form

$$\mathcal{A}_S^{[4]} = \{\gamma^\alpha\}d(q)\mathcal{A}_{S\alpha\beta}^{[4]}(q)d(q)\{\gamma^\beta\}\,; \tag{5.22}$$

then identify

$$\Im m\widehat{\Pi}_{\alpha\beta}^{(1)}(q) = \mathcal{A}_{S\alpha\beta}^{[4]}(q)\,. \tag{5.23}$$

From the last equation follows

$$\Im m\widehat{\Pi}_{\alpha\beta}(q) = \frac{1}{2}g^2 C_A\left[\Gamma_{F\alpha\mu\nu}^{(0)}(q,p_1,p_2)\Gamma_{F\beta}^{(0)\mu\nu}(q,p_1,p_2) - 2(p_2 - p_1)_\alpha(p_2 - p_1)_\beta\right]\,. \tag{5.24}$$

This last equation leads to a well-defined definition of $\widehat{\Pi}^{(1)}$, without having to resort to an intermediate one-loop diagrammatic interpretation: after the two-body phase space integrations has been carried out using standard results [13], the real parts may be reconstructed by means of a once-subtracted dispersion relation. Thus, in the absence of a full (dispersive) one-loop construction, the $\widehat{\Pi}^{(1)}$ so generated does not necessarily have to correspond to the imaginary parts of a precisely identifiable set of one-loop Feynman diagrams. Of course, given that the full one-loop construction has been carried out, we know that this is actually the case. Thus, when the one-loop (or n-loop) construction for $\widehat{\Pi}$ exists, Eq.(5.22) reduces into a non-trivial self-consistency check. In particular, one must verify that

$$\mathcal{A}_{S\alpha\beta}^{[4]}(q) = \mathcal{C}_2\left\{\widehat{\Pi}_{\alpha\beta}^{(1)}(q)\right\} = \mathcal{C}_2\left\{\widetilde{\Pi}_{\alpha\beta}^{(1)}(q, \xi_Q = 1)\right\}\,, \tag{5.25}$$

where $\mathcal{C}_n\{...\}$ is the operator which carries out the n-particle Cutkosky cuts (for $n = 2$ we have two-gluon and two-ghost cuts) to the quantity appearing inside the curly bracket (Fig.15). This is indeed the case [13], as can be directly verified from Eq.(2.17). In fact, the residual contributions originating from the terms proportional to p_1^μ and p_2^ν mentioned above correspond precisely to the Cutkosky cuts of the one-loop ghost diagrams (Fig.15b).

To fully appreciate the subtlety of the above construction the following comments are now in order:

(i) Of course, the BRS-driven cancellation for the process $q\bar{q} \to gg$ takes place regardless of the PT rearrangement of the amplitude in general, and the PT decomposition of $\Gamma^{(0)}_{\alpha\mu\nu}$ in particular. Indeed, if we had not eliminated $\Gamma^{(0)}_{P\alpha\mu\nu}(q, p_1, p_2)$ but had kept instead the full vertex $\Gamma^{(0)}_{\alpha\mu\nu}(q, p_1, p_2)$ (as is usually done), the WI analogous to Eq. (5.16) would be simply

$$p_1^\mu \Gamma^{(0)}_{\alpha\mu\nu}(q, p_1, p_2) = t_{\alpha\nu}(q) - t_{\alpha\nu}(p_2),$$
$$p_2^\nu \Gamma^{(0)}_{\alpha\mu\nu}(q, p_1, p_2) = t_{\alpha\mu}(p_1) - t_{\alpha\mu}(q). \qquad (5.26)$$

The parts which participate in the BRS cancellation, namely the parts proportional to $t_{\alpha\nu}(q)$ and $t_{\alpha\mu}(q)$ are thus unaffected. What changes after the PT rearrangement is the resulting absorptive part of the effective n-point functions under construction. So, if one was to define the absorptive part of an effective self-energy keeping the full $\Gamma^{(0)}_{\alpha\mu\nu}(q, p_1, p_2)$, but still exploiting the BRS cancellation in order to elliminate the longitudial terms, one would arrive at the imaginary part of the conventional self-energy in the RFG, $\Im m \Pi_{\alpha\beta}(q)$; the latter, for one thing, does not capture the running of the QCD coupling.

(ii) One could define the absorptive part of an effective self-energy before carrying out the BRS cancellation. In that case one would be led to the absorptive parts of the gluon self-energy in the light-cone gauges; in particular, the final answer would depend explicitly on the unphysical quantities n and η. A dispersion relation would give rise to a pathological quantity, since the gluon self-energy computed within the axial gauges is not multiplicatively renormalizable, due to its dependence on n_α [47]. Furthermore, spurious infrared divergences appear in the Feynman parameter integrations, which are artifacts and cancel out only when full physical quantities are computed [48].

Thus, one has to first carry out the PT rearrangement at the level of the S-matrix element, then enforce the BRS cancellation at the level of the cross-section, and, only after these two steps, one should define self-energy/vertex/box absorptive parts, as one would for a scalar field theory.

Having set up the formalism and discussed the general methodology, we next proceed with the two-loop absorptive construction.

VI. THE TWO-LOOP ABSORPTIVE CONSTRUCTION

In this section we will show how to extend the methodology established in the previous section to the two-loop case. This construction involves two parts: the first part is the study of the one-loop amplitude for the process $q(k_1)\bar{q}(k_2) \to g(p_1)g(p_2)$; the second is the study of the tree-level process $q(k_1)\bar{q}(k_2) \to g(p_1)g(p_2)g(p_3)$. As we will see in detail the PT rearrangement (at the level of the S-matrix), will give rise (at the level of the cross-section) to the correct Cutkosky cuts.

A. The one-loop version of $\Gamma_F^{(0)}$ and $\Gamma_P^{(0)}$

In this sub-section we will first study the conventional one-loop three-gluon vertex, and will see how one can arrive at the one-loop generalization of the tree-level vertices $\Gamma^{(0)}_{F\alpha\mu\nu}$ and $\Gamma^{(0)}_{P\alpha\mu\nu}$, defined in Eq.(2.3), to be denoted by $\Gamma^{(1)}_{F\alpha\mu\nu}$ and $\Gamma^{(1)}_{P\alpha\mu\nu}$, respectively. Then we will see in detail why casting the one-loop S-matrix for the process $q(k_1)\bar{q}(k_2) \to g(p_1)g(p_2)$ into its PT form is crucial for enforcing the optical theorem at the level of *individual* two-loop PT Green's functions.

We start with the one-loop S-matrix element for $q(k_1)\bar{q}(k_2) \to g(p_1)g(p_2)$.

Then Eq. (5.15) yields ($k = 4$)

$$p_1^\mu \left(\mathcal{T}^{[4]F}_{2s} + \mathcal{T}^{[4]F}_{2t} \right)^{ab}_{\mu\nu} = \left(S^{[4]F\{12\}}_{2s} + S^{[4]F\{12\}}_{2t} \right)^{ab} p_{2\nu}, \qquad (6.27)$$

where $\mathcal{T}_{2s}^{[4]F}$ and $\mathcal{T}_{2t}^{[4]F}$ are the "Feynman" versions of $\mathcal{T}_{2s}^{[4]}$ and $\mathcal{T}_{2t}$; their exact form will be specified shortly. The last two equations in (5.17) become

$$p_1^\mu (\mathcal{T}_{2s}^{[4]F})_{\mu\nu}^{ab} = (S_{2s}^{[4]F\{12\}})^{ab} p_{2\nu} + (\Lambda_2^{[4]F})_\nu^{ab},$$
$$p_1^\mu (\mathcal{T}_{2t}^{[4]F})_{\mu\nu}^{ab} = (S_{2t}^{[4]F\{12\}})^{ab} p_{2\nu} - (\Lambda_2^{[4]F})_\nu^{ab}. \qquad (6.28)$$

Using Eq.(5.19), we have that

$$\mathcal{A}_2^{[6]} = \left(\frac{1}{2!}\right) \Re e \left[\left(\mathcal{T}_{2s}^{[4]F} + \mathcal{T}_{2t}^{[4]F}\right) \left(\mathcal{T}_{2s}^{[2]F} + \mathcal{T}_{2t}^{[2]}\right)^* - 2\left(S_{2s}^{[4]F\{12\}} + S_{2t}^{[4]F\{12\}}\right) \left(S_{2s}^{[2]F\{21\}}\right)^* \right]$$
$$= \mathcal{A}_{2S}^{[6]} + \mathcal{A}_{2V}^{[6]} + \mathcal{A}_{2B}^{[6]}, \qquad (6.29)$$

with

$$\mathcal{A}_{2S}^{[6]} = \left(\frac{1}{2!}\right) \Re e \left[\mathcal{T}_{2s}^{[4]F} \mathcal{T}_{2s}^{[2]F^*} - 2\left(S_{2s}^{[4]F\{12\}}\right) \left(S_{2s}^{[2]F\{21\}}\right)^* \right],$$
$$\mathcal{A}_{2V}^{[6]} = \left(\frac{1}{2!}\right) \Re e \left[\mathcal{T}_{2s}^{[4]F} \mathcal{T}_{2t}^{[2]^*} + \mathcal{T}_{2s}^{[2]F} \mathcal{T}_{2t}^{[4]F^*} - 2\left(S_{2s}^{[2]F\{12\}}\right) \left(S_{2t}^{[4]F\{21\}}\right)^* \right],$$
$$\mathcal{A}_{2B}^{[6]} = \left(\frac{1}{2!}\right) \Re e \left[\mathcal{T}_{2t}^{[4]F} \mathcal{T}_{2t}^{[2]^*} \right]. \qquad (6.30)$$

From these last quantities one could define, for example, the quantity $\mathcal{A}_{2S\alpha\beta}^{[6]}(q)$ exactly as in Eq. (5.22), i.e.

$$\mathcal{A}_{2S}^{[6]} = \{\gamma^\alpha\} d(q) \mathcal{A}_{2S\alpha\beta}^{[6]}(q) d(q) \{\gamma^\beta\} \qquad (6.31)$$

The $\mathcal{A}_{2S\alpha\beta}^{[6]}(q)$ must then be such that

$$\mathcal{A}_{2S\alpha\beta}^{[6]}(q) = \mathcal{C}_2 \left\{ \widehat{\Pi}_{\alpha\beta}^{(2)}(q) \right\} = \mathcal{C}_2 \left\{ \widetilde{\Pi}_{\alpha\beta}^{(2)}(q, \xi_Q = 1) \right\} \qquad (6.32)$$

The question is what is the correct form of $\mathcal{T}_{2s}^{[4]}$ and $\mathcal{T}_{2t}^F$, and the corresponding $S_{2s}^{[2]F\{12\}}$ and $S_{2s}^{[2]F\{12\}}$; the latter quantities are automatically determined once the former have been specified. In particular, if such a rearrangement exist, does it correspond to a structure already known from the one-loop PT analysis ? The natural candidate for this is clearly the PT rearranged one-loop matrix element for $q(k_1)\bar{q}(k_2) \to g(p_1)g(p_2)$, shown in Fig.16 (individual Feynman graphs are shown in Fig.17, Fig.18, and Fig.19); if that were the case, one would begin to discern an iterative pattern. As we will see in detail, this is indeed what happens.

Throughout this section we will suppress the one-loop integration symbol $\int [dk]$, and will use (see Eq. (2.9))

$$J_3 \equiv J_3(q, -p_1, k) = \frac{i}{2} g^2 C_A [k^2 (k-p_1)^2 (k+p_2)^2]^{-1}. \qquad (6.33)$$

We focus on the part of the process involving the conventional one-loop three-gluon vertex $\Gamma_{\alpha\mu\nu}^{(1)}(q, p_1, p_2)$, which is diagrammatically shown in Fig.17 . Let us now carry out the decomposition of Eq. (2.2) to the elementary three-gluon vertex $\Gamma_{\alpha\sigma\rho}^{(0)}(q, k+p_2, -k+p_1)$ appearing in the diagrams of Fig.17a and Fig.17d; the parts stemming from the $\Gamma_{P\alpha\sigma\rho}^{(0)}$ will propagate towards the remaining elementary three-and four gluon vertices, and will trigger further WI of the type shown in Eq. (5.26). Reorganizing the terms thusly generated, one can show that the $\Gamma_{\alpha\mu\nu}^{(1)}(q, p_1, p_2)$ of Fig.17 can be written in the form

$$\Gamma_{\alpha\mu\nu}^{(1)}(q, p_1, p_2) = \left[\frac{1}{2} \Pi_{P\alpha\beta}^{(1)}(q)\right] d(q) \Gamma_{F\ \mu\nu}^{(0)\beta}(q, p_1, p_2) + \Gamma_{F\ \alpha\mu\nu}^{(1)}(q, p_1, p_2) + \Gamma_{P\ \alpha\mu\nu}^{(1)}(q, p_1, p_2), \qquad (6.34)$$

with

$$\Gamma^{(1)}_{P\,\alpha\mu\nu}(q,p_1,p_2) = -t^\rho_\mu(p_1)J_3\left[\Gamma^{(0)}_{\nu\rho\alpha}(p_2,k,-k-p_2)+k_\nu g_{\alpha\rho}\right]$$
$$-t^\rho_\nu(p_2)J_3\left[\Gamma^{(0)}_{\mu\alpha\rho}(p_1,k-p_1,-k)+k_\mu g_{\alpha\rho}\right]$$
$$-\frac{i}{2}V^{(1)}_{P\alpha\beta}\Gamma^{(0)\beta}_{P\mu\nu}(q,p_1,p_2)+\frac{1}{2}d(q)(p_2^2-p_1^2)\,q_\alpha V^{(1)}_{P\mu\nu}(q)\,. \tag{6.35}$$

The first term is precisely half of the pinch contribution needed for converting $\Pi^{(1)}_{\alpha\nu}(q)$ into $\widehat{\Pi}^{(1)}_{\alpha\nu}(q)$, as shown in Fig.16a; the other half will come from the one-loop quark-gluon vertex shown in Fig.19d, following the usual one-loop PT procedure presented in section II. This part of the construction has been first carried out in [49], where the process-independence of the $\widehat{\Pi}^{(1)}_{\alpha\nu}(q)$ was explicitly demonstrated.

The second term, $\Gamma^{(1)}_{P\,\alpha\mu\nu}(q,p_1,p_2)$, is Bose-symmetric with respect to $p_1 \leftrightarrow p_2$. As one can easily verify from Eq. (6.35), $\Gamma^{(1)}_{P\,\alpha\mu\nu}(q,p_1,p_2)$ is zero on shell, i.e. when contracting with the polarization tensors and using $p_1^2 = p_1^2 = 0$. Thus $\Gamma^{(1)}_{P\,\alpha\mu\nu}(q,p_1,p_2)$ can be dropped when studying the one-loop process $q\bar{q} \to gg$, exactly as $\Gamma^{(0)}_{P\,\alpha\mu\nu}(q,p_1,p_2)$ was dropped in the tree-level case. As we we have seen in section IIIB, in the off-shell case, i.e. when $\Gamma^{(1)}_{\alpha\mu\nu}(q,p_1,p_2)$ is inserted into a two-loop quark-gluon vertex, the parts proportional to p_1^μ and p_2^ν pinch the internal quark propagator and give propagator-like contributions, whereas the parts proportional to p_1^2 and p_2^2 cancel exactly against analogous contributions from the rest of the graphs contributing to the two-loop quark-gluon vertex. Finally, $\Gamma^{(1)}_{F\,\alpha\mu\nu}(q,p_1,p_2)$, is exactly the one-loop version of $\Gamma^{(0)}_{F\,\alpha\mu\nu}(q,p_1,p_2)$: It is the one-loop three-point function involving one background (q) and two quantum (p_1,p_2) gluons as incoming fields, computed using the BFMFG Feynman rules. (Fig.18). Notice that the special ghost structure characteristic of the BFM (Fig.18e – Fig.18h) emerges *automatically*, after following the procedure outlined above.

It is straightforward to show that $\Gamma^{(1)}_{F\,\alpha\mu\nu}(q,p_1,p_2)$ satisfies the following WI

$$q^\alpha \Gamma^{(1)}_{F\,\alpha\mu\nu}(q,p_1,p_2) = \Pi^{(1)}_{\mu\nu}(p_1) - \Pi^{(1)}_{\mu\nu}(p_2), \tag{6.36}$$

which is the exact one-loop analogue of the tree-level Ward identity of Eq (2.4); indeed the RHS is the difference of two conventional one-loop self-energies computed in the RFG.

In addition, we have for the action of $p_{1\mu}$ on $\Gamma^{(1)}_{F\,\alpha\mu\nu}(q,p_1,p_2)$ when $p_1^2 = p_2^2 = 0$, is given by

$$p_1^\mu \Gamma^{(1)}_{F\,\alpha\mu\nu} = i\widehat{\Pi}^{(1)}_{\alpha\nu}(q) - i\Pi^{(1)}_{\alpha\nu}(p_2) + \lambda^{(1)}_{\nu\sigma}t^\sigma_\alpha(q) + s^{(1)}_\alpha p_{2\nu} \tag{6.37}$$

where $\widehat{\Pi}^{(1)}_{\alpha\nu}(q)$ is given in Eq (2.14), and

$$\lambda^{(1)}_{\nu\sigma} = J_3\left[(k-p_1)^\rho\Gamma^{(0)}_{\nu\rho\sigma}(p_2,k,-k-p_2)-(k+p_2)_\nu k_\sigma\right]-i\left[2B(q)+B(p_1)\right]g_{\nu\sigma} \tag{6.38}$$

$$s^{(1)}_\alpha = J_3\left[p_2^\sigma k^\rho \Gamma^{(0)}_{F\alpha\sigma\rho}(q,k+p_2,-k+p_1)-p_2\cdot(k-p_1)(2k+p_2-p_1)_\alpha\right]$$
$$+\left(\frac{1}{8}\right)\left[B(p_1)+B(p_2)\right]q_\alpha \tag{6.39}$$

with

$$B(p) \equiv \int[dk]J_1(p,k)\,. \tag{6.40}$$

Eq. (6.37) is the one-loop analogue of Eq. (5.16). It is important to emphasize that $\Gamma^{(1)}_{F\,\alpha\mu\nu}(q,p_1,p_2)$ is *not* equal to the one-loop PT three-gluon vertex $\widehat{\Gamma}^{(1)}_{\alpha\mu\nu}(q,p_1,p_2)$ constructed in [3]. Notice also that, unlike the tree-level case, now there will be a t-channel ghost (we will not report its closed expression here) and that the t-channel has been modified also in order to achieve the PT one-loop rearrangement.

Thus we have,

$$\mathcal{T}^{[4]F}_{2s} = (16a) + (16b) + (16d) + (16e) \tag{6.41}$$

20

with (we suppress a common factor $g\{\gamma^e_\alpha\}f^{eab}d(q)$)

$$(16b) = \Gamma^{(1)}_{F\alpha\mu\nu}(q,p_1,p_2)\,,$$
$$(16a) = \widehat{\Pi}^{(1)}_{\alpha\sigma}(q)d(q)\Gamma^{(0)\sigma}_{F\ \mu\nu}(q,p_1,p_2)\,,$$
$$(16d) = \Gamma^{(0)}_{F\alpha\mu\sigma}(q,p_1,p_2)d(p_2)\Pi^{(1)\sigma}_\nu(p_2)\,,$$
$$(16e) = \Gamma^{(0)}_{F\alpha\sigma\nu}(q,p_1,p_2)d(p_1)\Pi^{(1)\sigma}_\mu(p_1) \tag{6.42}$$

and so, together with the first equation in (5.17)

$$\mathcal{T}^{[4]F}_{2s}\mathcal{T}^{[2]F*}_{2s} = \Bigg((16b)+(16d)+(16e)\Bigg)\cdot\mathcal{T}^{[2]F*}_{2s} + (16a)\cdot\mathcal{T}^{[2]F*}_{2s}$$

$$= \Bigg((20a)+(20b)+(20d)+(20f)+(20j)+(20g)+(20h)\Bigg) + \mathcal{C}_{2gluons}\Big\{(4e)\Big\} \tag{6.43}$$

i.e. we recover the two-gluon Cutkosky cuts of $\widetilde{\Pi}^{(2)}_{\alpha\beta}(q,\xi_Q=1)$ (Fig.20), together with the corresponding two-gluon cuts of the 1PR graph in Fig.4e, as we should. To account for the remaining two-ghost Cutkosky cuts in Fig.20 and Fig.4e we need, in addition to Eq. (6.37), the following results

$$p_1\cdot(16a) = -i\widehat{\Pi}^{(1)}_{\alpha\nu}(q) + \widehat{\Pi}^{(1)}_{\alpha\sigma}(q)d(q)(p_2-p_1)^\sigma p_{2\nu}\,,$$
$$p_1\cdot(16d) = t_{\alpha\sigma}(q)\Pi^{(1)\sigma}_\nu(p_2) + i\Pi^{(1)}_{\alpha\nu}(p_2)\,,$$
$$p_1\cdot(16e) = 0\,. \tag{6.44}$$

Then we have

$$p_1\cdot\Bigg((16a)+(16b)+(16d)+(16e)\Bigg) = t^\sigma_\alpha(q)\Bigg(\lambda^{(1)}_{\nu\sigma}+\Pi^{(1)}_{\sigma\nu}(p_2)\Bigg)$$

$$+\Bigg(s^{(1)}_\alpha+\widehat{\Pi}^{(1)}_{\alpha\sigma}(q)d(q)(p_2-p_1)^\sigma\Bigg)p_{2\nu} \tag{6.45}$$

From the above results one may immediately deduce the closed form of $(\Lambda^{[4]F}_2)^{ab}_\nu$ and $\left(S^{[4]F\{12\}}_{2s}\right)^{ab}$ appearing in Eq. (6.28):

$$\left(S^{[4]F\{12\}}_{2s}\right)^{ab} = g\{\gamma^e_\alpha\}f^{eab}d(q)\Bigg(s^{(1)}_\alpha+\widehat{\Pi}^{(1)}_{\alpha\sigma}(q)d(q)(p_2-p_1)^\sigma\Bigg)$$

$$(\Lambda^{[4]F}_2)^{ab}_\nu = -ig\{\gamma^e_\alpha\}f^{eab}\Bigg(\lambda^{(1)\alpha}_\nu+\Pi^{(1)\alpha}_\nu(p_2)\Bigg) \tag{6.46}$$

Then we have

$$2S^{[4]F\{12\}}_{2s}S^{[4]F\{21\}}_{2s} = 2s^{(1)}_\alpha(p_2-p_1)_\beta + 2\widehat{\Pi}^{(1)}_{\alpha\sigma}(q)(p_2-p_1)_\sigma(p_2-p_1)_\beta$$

$$= \Bigg((20i)+(20e)+(20m)+(20n)+(20q)+(20r)\Bigg) + \mathcal{C}_{2ghosts}\Big\{(4e)\Big\} \tag{6.47}$$

which concludes the proof of Eq (6.32).

B. Tree-level $q(k_1)\bar{q}(k_2)\to g(p_1)g(p_2)g(p_3)$, and the $\Gamma^{(0)}_{F\alpha\mu\nu\rho}(q,p_1,p_2,p_3)$

Next we consider the tree-level amplitude for the process $q(k_1)\bar{q}(k_2)\to g(p_1)g(p_2)g(p_3)$, shown in Fig.21 . This amplitude must be appropriately rearranged, and it will eventually furnish the imaginary parts corresponding to the three-particle Cutkosky cuts of $\widehat{\Pi}^{(2)}(q)$.

21

We start by presenting some general properties of this amplitude. It is straightforward to verify that $\mathcal{T}^{abc}_{\mu\nu\rho}$ satisfies the following identities:

$$p_1^\mu \mathcal{T}^{abc}_{3\mu\nu\rho} = (S_3^{\{12\}})^{abc}_\rho p_{2\nu} + (S_3^{\{13\}})^{abc}_\nu p_{3\rho},$$
$$p_2^\nu \mathcal{T}^{abc}_{3\mu\nu\rho} = (S_3^{\{21\}})^{abc}_\rho p_{1\mu} + (S_3^{\{23\}})^{abc}_\mu p_{3\rho},$$
$$p_3^\rho \mathcal{T}^{abc}_{3\mu\nu\rho} = (S_3^{\{31\}})^{abc}_\nu p_{1\mu} + (S_3^{\{32\}})^{abc}_\mu p_{2\nu}. \tag{6.48}$$

Bose symmetry imposes the following relations among the $S_3^{\{ij\}}$ amplitudes [35]:

$$(S_3^{\{ij\}})^{a_i a_j a_\ell}_\sigma (p_i, p_j, p_\ell) = (S_3^{\{ji\}})^{a_j a_i a_\ell}_\sigma (p_j, p_i, p_\ell)$$
$$(S_3^{\{ij\}})^{a_i a_j a_\ell}_\sigma (p_i, p_j, p_\ell) = (S_3^{\{i\ell\}})^{a_i a_\ell a_j}_\sigma (p_i, p_\ell, p_j), \tag{6.49}$$

and

$$p_i^\sigma (\mathcal{S}^{\{j\ell\}})^{abc}_\sigma = p_j^\sigma (\mathcal{S}^{\{i\ell\}})^{abc}_\sigma, \quad \ell \neq i \neq j. \tag{6.50}$$

These sets of identities guarantee that all dependence on the unphysical four-vector n_α and the gauge parameter η appearing in the polarization tensors will disappear from the final expression for $\mathcal{A}_3^{[6]}$.

The amplitude rearrangement is as follows (Fig.21):

$$(\mathcal{T}_{3s}^{[3]F})^{abc}_{\mu\nu\rho} = g^2 \{\gamma^{e,\alpha}\} d(q) \Gamma_{F\alpha\mu\nu\rho}^{(0)eabc}(q, p_1, p_2, p_3)$$
$$(\mathcal{T}_{3t}^{[3]F})^{abc}_{\mu\nu\rho} = (\mathcal{T}_{3t}^{[3]})^{abc}_{\mu\nu\rho} \tag{6.51}$$

where

$$\Gamma_{F\alpha\mu\nu\rho}^{(0)eabc}(q, p_1, p_2, p_3) = f^{ecx} f^{abx} d(p_1 + p_2) \Gamma_{F\alpha\rho\sigma}^{(0)}(q, p_3, p_1 + p_2) \Gamma_{\mu\nu}^{(0)\sigma}(p_1, p_2, -p_1 - p_2)$$
$$+ f^{ebx} f^{acx} d(k_1 + k_3) \Gamma_{F\alpha\nu}^{(0)}(q, p_2, p_1 + p_3) \Gamma_{\mu\rho\sigma}^{(0)\sigma}(p_1, p_3, -p_1 - p_3)$$
$$+ f^{eax} f^{bcx} d(k_2 + k_3) \Gamma_{F\alpha\mu\sigma}^{(0)}(q, p_1, p_2 + p_3) \Gamma_{\nu\rho}^{(0)\sigma}(p_2, p_3, -p_2 - p_3)$$
$$+ \Gamma_{\alpha\mu\nu\rho}^{(0)eabc} \tag{6.52}$$

It is easy to verify now that $\Gamma_{F\alpha\mu\nu\rho}^{(0)eabc}(q, p_1, p_2, p_3)$ is the analogue of $\Gamma_{F\alpha\mu\nu}^{(0)abc}(q, p_1, p_2)$ appearing in the first equation of (5.17) for the case of three on-shell gluons. In particular, we have that

$$q^\alpha \Gamma_{F\alpha\mu\nu\rho}^{(0)eabc}(q, p_1, p_2, p_3) = -f^{ecx} f^{abx} p_3^2 d(p_1 + p_2) \Gamma_{\mu\nu\rho}^{(0)}(p_1, p_2, -p_1 - p_2)$$
$$- f^{ebx} f^{acx} p_2^2 d(k_1 + k_3) \Gamma_{\mu\rho\nu}^{(0)}(p_1, p_3, -p_1 - p_3)$$
$$- f^{eax} f^{bcx} p_1^2 d(k_2 + k_3) \Gamma_{\nu\rho\mu}^{(0)}(p_2, p_3, -p_2 - p_3), \tag{6.53}$$

where we have used the well-known WI relating the bare three-and four-gluon vertices [36]. Eq. (6.53) is the analogue of Eq. (2.4). Clearly, when $p_1^2 = p_2^2 = p_3^2 = 0$,

$$q^\alpha \Gamma_{F\alpha\mu\nu\rho}^{(0)eabc}(q, p_1, p_2, p_3) = 0, \tag{6.54}$$

exactly as happens in Eq. (2.4).

In addition,

$$p_1^\mu (\mathcal{T}_{3s}^{[3]F})^{abc}_{\mu\nu\rho} = (S_{3s}^{[3]F\{12\}})^{abc}_\rho p_{2\nu} + (S_{3s}^{[3]F\{13\}})^{abc}_\nu p_{3\rho} + (\Lambda_3^{[3]F})^{abc}_{\nu\rho},$$
$$p_1^\mu (\mathcal{T}_{3t}^{[3]})^{abc}_{\mu\nu\rho} = (S_{3t}^{[3]\{12\}})^{abc}_\rho p_{2\nu} + (S_{3t}^{[3]\{13\}})^{abc}_\nu p_{3\rho} - (\Lambda_3^{[3]F})^{abc}_{\nu\rho} \tag{6.55}$$

where

$$(S_{3s}^{[3]F\{12\}})^{abc}_\rho = \{\gamma^{m,\alpha}\} d(q) \left[(Z_1)^{mabc}_{\alpha\rho} + (Z_2)^{mabc}_{\alpha\rho} + (Z_3)^{mabc}_{\alpha\rho} \right] \tag{6.56}$$

with

$$(Z_1)^{mabc}_{\alpha\rho} = g^2 f^{mcx} f^{abx} d(p_1+p_2) p_2^\sigma \Gamma^{(0)}_{F\alpha\rho\sigma}(q,p_3,p_1+p_2)$$

$$(Z_2)^{mabc}_{\alpha\rho} = g^2 f^{mbx} f^{acx} \left[d(p_1+p_3)(2p_2+q)_\alpha (p_1+p_3)_\rho - g_{\alpha\rho} \right]$$

$$(Z_3)^{mabc}_{\alpha\rho} = g^2 f^{max} f^{bcx} d(p_2+p_3)(2p_1+q)_\alpha p_{2\rho} \tag{6.57}$$

and

$$(S^{[3]\{12\}}_{3t})^{abc}_\rho = -g^3 \bar{v}(k_2) \left[\tau^c \gamma_\rho \, S(k_2+p_3) \, \tau^e \gamma_\sigma + \tau^e \gamma_\sigma \, S(k_1+p_3) \, \gamma_\rho \tau^c \right] u(k_1) f^{eab} d(p_1+p_2) p_2^\sigma. \tag{6.58}$$

Armed with the above relations, it is then straightforward to show that

$$\mathcal{A}^{[6]} = \frac{1}{2}\left(\frac{1}{3!}\right)\left[\left(\mathcal{T}^{[3]F}_{3s} + \mathcal{T}^{[3]}_{3t}\right)\left(\mathcal{T}^{[3]F}_{3s} + \mathcal{T}^{[3]}_{3t}\right)^* - 6\left(S^{[3]F\{12\}}_{3s} + S^{[3]\{12\}}_{3t}\right)\left(S^{[3]F\{21\}}_{3s} + S^{[3]\{21\}}_{3t}\right)^* \right]$$

$$= \mathcal{A}^{[6]}_S + \mathcal{A}^{[6]}_V + \mathcal{A}^{[6]}_B, \tag{6.59}$$

with

$$\mathcal{A}^{[6]}_S = \frac{1}{2}\left(\frac{1}{3!}\right)\left[\mathcal{T}^{[3]F}_{3s} \mathcal{T}^{[3]F*}_{3s} - 6\left(S^{[3]F\{12\}}_{3s}\right)\left(S^{[3]F\{21\}}_{3s}\right)^* \right],$$

$$\mathcal{A}^{[6]}_V = \frac{1}{2}\left(\frac{1}{3!}\right)\left[\left\{ \mathcal{T}^{[3]F}_{3s}\mathcal{T}^{[3]*}_{3t} - 6\left(S^{[3]F\{12\}}_{3s}\right)\left(S^{[3]\{21\}}_{3t}\right)^* \right\} + \left\{ \mathcal{T}^{[3]}_{3t}\mathcal{T}^{[3]F*}_{3s} - 6\left(S^{[3]\{12\}}_{3t}\right)\left(S^{[3]F\{21\}}_{3s}\right)^* \right\} \right],$$

$$\mathcal{A}^{[6]}_B = \frac{1}{2}\left(\frac{1}{3!}\right)\left[\mathcal{T}^{[3]}_{3t}\mathcal{T}^{[3]*}_{3t} - 6\left(S^{[3]F\{12\}}_{3t}\right)\left(S^{[3]\{21\}}_{3t}\right)^* \right], \tag{6.60}$$

We are now in position to prove that, indeed,

$$\mathcal{A}^{[6]}_{S\alpha\beta}(q) = \mathcal{C}_3\left\{ \widehat{\Pi}^{(2)}_{\alpha\beta}(q) \right\} = \mathcal{C}_3\left\{ \widetilde{\Pi}^{(2)}_{\alpha\beta}(q,\xi_Q = 1) \right\}, \tag{6.61}$$

where $\mathcal{A}^{[6]}_{S\alpha\beta}(q)$ is defined from $\mathcal{A}^{[6]}_S$ exactly as in Eq. (5.22) and Eq. (6.31).

To begin with,

$$\left(\frac{1}{12}\right)\mathcal{T}^{[3]F}_{3s}\mathcal{T}^{[3]F*}_{3s} = (22a)_{c_1} + (22a)_{c_2} + (22b) + (22c) + (22g) + (22\ell). \tag{6.62}$$

For the cuts involving ghosts we need the closed form of $S^{[3]F\{21\}}_{3s}$, which can be obtained from $S^{[3]F\{12\}}_{3s}$ of Eq. (6.57) by virtue of the relations given in Eq. (6.49). In particular,

$$(Z'_1)^{nabc}_{\beta\rho} = g^2 f^{ncr} f^{bar} d(p_1+p_2) p_1^\lambda \Gamma^{(0)}_{F\beta\rho\lambda}(q,p_3,p_1+p_2)$$

$$(Z'_2)^{nabc}_{\beta\rho} = g^2 f^{nar} f^{bcr} \left[d(p_2+p_3)(2p_1+q)_\beta (p_2+p_3)_\rho - g_{\beta\rho} \right]$$

$$(Z'_3)^{nabc}_{\beta\rho} = g^2 f^{nbr} f^{acr} d(p_1+p_3)(2p_2+q)_\beta p_{1\rho}. \tag{6.63}$$

Then it is straightforward to show that

$$\frac{1}{2} Z_1 Z'_1 = (22h),$$

$$\frac{1}{2} Z_1 Z'_2 = (22e)_{c_2} + (22k),$$

$$\frac{1}{2} Z_1 Z_3' = (22e)_{c_1} \,,$$

$$\frac{1}{2} Z_2 Z_1' = (22f)_{c_1} + (22j) \,,$$

$$\frac{1}{2} Z_2 Z_2' = (22i)_{c_1} + (22s) + (22n) + (22o) \,,$$

$$\frac{1}{2} Z_2 Z_3' = (22q) + (22m) \,,$$

$$\frac{1}{2} Z_3 Z_1' = (22f)_{c_2} \,,$$

$$\frac{1}{2} Z_3 Z_2' = (22r) + (22p) \,,$$

$$\frac{1}{2} Z_3 Z_3' = (22i)_{c_2} \,. \tag{6.64}$$

Thus, we have accounted for all three-particle Cutkosky cuts appearing in Fig.22 .

VII. DISCUSSION AND CONCLUSIONS

In this paper we have presented the generalization of the PT to two-loops for the case of mass-less Yang-Mills theories. Two different, but complementary derivations have been presented. In the first derivation we have followed the diagrammatic approach employed in the one-loop case [1–3], and have shown how the PT properties are replicated in the next order. In the second we have pursued the dispersive PT construction established in [13,14] and have shown that the resulting structures are consistent with those derived with the first method. We emphasize that throughout this entire analysis we have maintained a diagrammatic interpretation of the various contributions. In particular, no sub-integrations had to be carried out. This additional feature renders the method all the more powerful, because unitarity is manifest, and can be easily verified by means of the Cutkosky cuts. The combination of the two methods constrains significantly the PT construction presented here, and restricts severely any possible deviations from it. The reader should be able to recognize, for example, that any rearrangement of the (internal) vertices of two-loop box-diagrams (for example, of the so-called "H-diagram" discussed in the second paper of [12]) cannot be reconciled with the arguments of the simultaneous two- and three-particle Cutkosky cuts presented in section VI. Whereas no strict proof has been given here that the PT construction developed in this paper is mathematically unique, we consider that as a very plausible possibility. Notice also that the appearance of characteristic one-loop structures inside the two-loop PT Green's functions suggests the onset of an iterative pattern, which may provide clues leading to the generalization of the PT algorithm to all orders in perturbation theory.

The generalization of the two-loop PT construction to the case of Yang-Mills theories with spontaneous symmetry breaking (Higgs mechanism) in general, and the electroweak sector of the Standard Model in particular, should proceed precisely according to the methodology presented in this paper. Except for the additional book-keeping complications stemming from the presence of gauge-boson masses (modifications of WI, appearance of seagull and tadpole terms, diagrams with would-be Goldstone bosons), no additional conceptual obstacles are expected.

The results of this paper clearly prove that the correspondence between PT and BFMFG [11] persists at two-loops. Notice that this proof is based on an a-posteriori comparison with a result established through the systematic diagrammatic rearrangement of the physical S-matrix computed in the renormalizable gauges, rather than on an a-priori formal derivation at the level of the BFM generating functional. It would be clearly important to reach a deeper understanding of what singles out the value $\xi_Q = 1$. One possibility would be to look for special properties of the BFM action at $\xi_Q = 1$ [50]. In such a case one could choose to avoid the complications arising from renormalization, since the correspondence is valid also for the super-renormalizable 3-d QCD.

Just as happened in the one-loop case, the two-loop PT self-energy defined here lends itself as an essential ingredient for the extension of the notion of the QCD effective charge [2,51,17] to two-loops (for a thorough discussion of the one-loop case see [17]), since it has precisely the same properties as the corresponding QED quantity, i.e. the vacuum polarization of the photon. First of all, the two-loop PT self-energy captures the leading logarithms of the theory, i.e. the prefactor of the logarithm is the second coefficient of the QCD β function. Second, by virtue of the the QED like WI given in Eq. (4.6) the combination $\alpha_{eff}(q, \mu) \sim g^2(\mu)\widehat{\Delta}(q/\mu)$, where $\widehat{\Delta}(q/\mu) = [1 - \widehat{\Pi}^{(1)}(q/\mu) - \widehat{\Pi}^{(2)}(q/\mu)]^{-1}$ is a renormalization group invariant quantity. Third, it has by construction the correct unitarity structure [14]. While the α_{eff} defined above appears as the obvious candidate, a detailed study needs be carried out in order to determine

whether or not there are any field-theoretical obstructions [52] which would prevent the realization of the two-loop construction corresponding to the QCD effective charge.

In this context notice also that the construction presented here determines uniquely the constant term of the two-loop effective charge (within a given renormalization scheme) [53]. To determine its actual value one should go beyond the two-loop calculation presented in [9], and compute the Feynman diagrams of Fig.9 keeping also constant terms [54]. Knowledge of this constant term is important when the QCD effective charge is used in the field of renormalon calculus; in particular, it would be free of the ambiguities infesting the estimates of the renormalon contributions to physical observables [17,55].

In addition, it is well-known [56] that if one was to compute the two-loop gluon self-energy in the context of the BFM keeping ξ_Q arbitrary, the resulting ξ_Q-dependent term would be a constant, i.e. it would not affect the coefficient of the logarithm. While in such a case the residual gauge-dependence could be thought of as a renormalization-scheme ambiguity, i.e. it could be re-absorbed in the wave-function renormalization of the (background) gluon, this is not possible when the gauge fields are massive. In that case unitarity is even more constraining; as is known from the studies on the one-loop electro-weak effective charges [13–15], the gauge-dependence affects non-trivially the analytic structure of the answer, giving rise to unphysical thresholds.

The calculations presented in section VI constitute the first dispersive derivation of the two-loop QCD β function. In this analysis we have made use of the one-to-one correspondence between the physical S-matrix elements and the Cutkosky cuts of the two-loop PT self-energy. This construction involves a very particular combination of one-loop (section VIA) and tree-level graphs (section VIB); in addition to furnishing the correct β function coefficient, a subtle cancellation of infrared divergences also takes place: while both sets of graphs are infrared divergent, they combine to give a infrared finite answer. This can be directly inferred from the simple observation that the Cutkosky cutting procedure we have employed amounts finally to the determination of the imaginary part of a single logarithm, namely that of the two-loop self-energy; the latter is infrared finite [57,58]. While the Cutkosky formalism furnishes an intuitive diagrammatic understanding and a valuable calculational short-cut, it would be interesting to reproduce the results of section IV without resorting to it. In particular one could study the precise cancellation mechanism of the infrared divergences using a proper infrared regularization scheme, and explicit expressions for the two- and three-gluon phase-space, which we have not needed here. In addition, it would be interesting to attempt a similar two-loop derivation using the formalism developed in [59], and study possible connections.

It has been often advocated that the non-perturbative QCD effects can be reliably captured at an inclusive level by means of an infrared finite quantity, which would constitute the extension of the perturbative QCD running coupling to low energy scales [60] Early results by Cornwall based on the study of *gauge invariant* Schwinger-Dyson equations [2] involving this quantity suggest that such a description can in fact be derived from first principles. According to this analysis, the self-interaction of gluons give rise to a dynamical gluon mass, while preserving at the same time the local gauge symmetry of the theory. The presence of the gluon mass saturates the running of the QCD coupling; so, instead of increasing indefinitely in the infrared as perturbation theory predicts, it "freezes" at a finite value [3,61]. It would be interesting to revisit this issue in the light of the results derived in the present paper. For example, one could study the structure of the gauge-invariant Schwinger-Dyson equation for the PT gluon self-energy, and in particular the way the PT three-gluon vertex $\widehat{\Gamma}^{(1)}$ enters in the PT gluon self-energy, using the two loop results as a guidance. In doing so one could hope to systematically improve on the analysis of [2], where the gauge-technique ansatz for the vertex was used. In this context one may find it advantageous to rewrite the vertex $\Gamma_F^{(1)}$ appearing inside the two-loop PT gluon self-energy in terms of $\widehat{\Gamma}^{(1)}$; one should then interpret the emerging residual terms as parts of the two-loop self-energy, even though they appear to be pinch-like [62], i.e. once the PT self-energy has been fixed it may be recast into a different form, but no pieces should be re-assigned to vertices or boxes.

Finally it would be interesting to pursue a connection with other field- or string-theoretical methods [63–67], either in order to acquire a more formal understanding of the PT, or in order to combine various attempts into a coherent framework.

[1] J.M. Cornwall, in *Proceedings of the French-American Seminar on Theoretical Aspects of Quantum Chromodynamics*, Marseille, France, 1981, edited J.W. Dash (Centre de Physique Théorique, Marseille, 1982).

[2] J.M. Cornwall, Phys. Rev. **D26**, 1453 (1982).

[3] J.M. Cornwall and J. Papavassiliou, Phys. Rev. **D40**, 3474 (1989).

[4] J. Papavassiliou, Phys. Rev. **D41**, 3179 (1990).

[5] G. Degrassi and A. Sirlin, Phys. Rev. **D46**, 3104 (1992);

[6] J. Papavassiliou, Phys. Rev. **D 50**, 5958 (1994).

[7] G. Degrassi, B. Kniehl, and A. Sirlin, Phys. Rev. **D48**, R3963 (1993); J. Papavassiliou and K. Philippides, Phys. Rev **D 48**, 4255 (1993); J. Papavassiliou and C. Parrinello, Phys. Rev **D 50**, 3059 (1994); K. Hagiwara, S. Matsumoto, D. Haidt, and C.S. Kim Z. Phys. **C64**, 559,(1994), Erratum-ibid. **C68**, 352 (1995); J. Papavassiliou, K. Philippides, and K. Sasaki, Phys.Rev.**D53**, 3942 (1996).

[8] B.S. DeWitt, *Phys. Rev.* **162**, 1195 (1967); G. 't Hooft, in *Acta Universitatis Wratislvensis no. 38*, 12th Winter School of Theoretical Physics in Kapacz, Functional and probabilistic methods in quantum field theory vol. I (1975); B.S. DeWitt, *A gauge invariant effective action*, in Quantum gravity II, ed. C. Isham, R. Penrose, and D. Sciama (Oxford press, 1981).

[9] L.F. Abbott, Nucl. Phys. **B185**, 189 (1981), and references therein.

[10] L.F. Abbott, M.T. Grisaru, and R.K. Schaeffer, Nucl. Phys. **B229**, 372 (1983).

[11] A. Denner, S. Dittmaier, and G. Weiglein, Phys. Lett. **B333**, 420 (1994); S. Hashimoto, J. Kodaira, Y. Yasui, and K. Sasaki, Phys. Rev. **D50**, 7066 (1994); E. de Rafael and N. J. Watson, unpublished.

[12] J. Papavassiliou and A. Pilaftsis, Phys. Rev. Lett. **75**, 3060 (1995); Phys. Rev. **D53**, 2128 (1996).

[13] J. Papavassiliou and A. Pilaftsis, Phys. Rev. **D54**, 5315 (1996).

[14] J. Papavassiliou, E. de Rafael, and N.J. Watson, Nucl. Phys. **B503**, 79 (1997).

[15] J. Papavassiliou and A. Pilaftsis, Phys. Rev. Lett. **80**, 2785 (1998); Phys. Rev. **D58** (1998):053002.

[16] G. Alexanian and V.P.Nair, Phys. Lett. **B352**, 435 (1995); K.Sasaki, Nucl.Phys. **B472** 271 (1996); *ibid* **B490**, 472 (1997).

[17] N.J. Watson, Nucl. Phys. **B494**, 388 (1997).

[18] S. Peris and E. de Rafael, Nucl. Phys. **B500** 325, (1997).

[19] A. Pilaftsis, Nucl. Phys. **B487**, 467 (1997).

[20] R.Cruz, B.Grzadkowski, and J.F.Gunion, Phys. Lett. **B289**, 440 (1992); D. Atwood, G. Eilam, A. Soni, R.R. Mendel, R. Migneron Phys. Rev. Lett. **70** 1364 (1993).

[21] A. Pilaftsis, Phys. Rev. Lett. **77**, 4996 (1996); Nucl. Phys. **B504**, 61 (1997).

[22] R. Kleiss and W. J. Stirling, Phys. Lett. **B182**, 75 (1986); U. Baur and E. W. N Glover, Nucl. Phys. **B347**, 12 (1990); Phys. Rev. **D44**, 99 (1991).

[23] K. Philippides and W.J. Stirling, Eur. Phys. J. **C9**, 181 (1999).

[24] See also D.C. Kennedy and B.W. Lynn, Nucl. Phys. **B322**, 1 (1989).

[25] J. Papavassiliou, *The Pinch Technique Approach to the Physics of Unstable Particles*, hep-ph/9905328, contribution to the 1998 Corfu Summer Institute on Elementary Particle Physics (JHEP proceedings).

[26] J. Papavassiliou, *The Pinch Technique at Two Loops*, hep-ph/9912336.

[27] N.J. Watson, Nucl.Phys.Proc.Suppl.74:341-344,1999.

[28] A. Slavnov, Theor. and Math. Phys. **10**, 99 (1973); J.C. Taylor, Nucl. Phys. **B33**, 436 (1971).

[29] G. 't Hooft, Nucl. Phys. **B33**, 173 (1971); J.M. Cornwall and G. Tiktopoulos, Phys. Rev. **D15**, 2937 (1977).

[30] J. Papavassiliou, Phys. Rev. **D51**, 856 (1995).

[31] M. Passera and K. Sasaki, Phys. Rev. **D54**, 5763 (1996)

[32] E. de Rafael and J.L. Rosner, Ann. Phys. (NY) **82**, 369 (1973)

[33] H.D. Politzer, Phys. Rev. Lett. **30**, 1346 (1973); D. Gross and F. Wilczek, Phys. Rev. Lett. **30**, 1343 (1973).

[34] T. Kunimasa and T. Goto, Prog. Theor. Phys. **37**, 452 (1967); A.A. Slavnov, Theor. Math. Phys. **10**, 305 (1972); J.M. Cornwall, Phys. Rev. **D10**, 500 (1974).

[35] J. R. Forshaw, J. Papavassiliou, and C. Parrinello, Phys. Rev. **D59**:074008 (1999).

[36] J. Papavassiliou, Phys. Rev **D47**, 4728 (1993).

[37] K. Philippides and A. Sirlin, Nucl. Phys. **B477**,59 (1996)

[38] The notion of "internal" and "external" three-gluon vertex can be generalized also to include the case where the gauge-invariant physical observable is not an S-matrix element, but instead a gauge-invariant Green's function. For example one could carry out the PT program inside the Green's function $G(x,y) = \langle 0|T(Tr\{\Phi(x)\Phi(x)^{\dagger}\}Tr\{\Phi(y)\Phi(y)^{\dagger}\}|0\rangle$, where $\Phi(x)$ is a matrix describing a set of scalar test particles in an appropriate representation of the gauge group; this latter quantity was employed by Cornwall for the original PT construction [2]. In that case the "external" momentum is the momentum transfer between the two sides of the scalar loop, i.e., as explained in [2], one should count loops as if the Φ loop were opened at x and y.

[39] For an attempt to define the 2-loop PT quark self-energy by modifying its internal three-gluon vertices see N.J. Watson,

Nucl. Phys. **B552**, 461 (1999) .

[40] W. Buchmüller and O. Philipsen, Phys. Lett. **B397**, 112 (1997); R. Jackiw and S.-Y. Pi, Phys. Lett. **B 403**, 297 (1997); J.M. Cornwall, Phys. Rev. **D57**, 3694 (1998); Phys. Rev. **D59** (1999):125015.

[41] W.E. Caswell, Phys. Rev. Lett. **33**, 1346 (1973).

[42] D.R.T. Jones, Nucl. Phys. **B75**, 531 (1974).

[43] At one loop one can verify these relations explicitly by computing the divergent part of $V_P^{(1)}$ in Eq. (2.12), together with the expressions for the various one-loop renormalization constants listed in Eq.5 – Eq.7 of [42] (notice the difference in the notation, and that $d = 4 - \epsilon$)

[44] We will not consider the case where one has quarks as intermediate states; it can be straightforwardly deduced from the gluonic case. In fact, one should be able to verify easily that the absorptive construction in this case is in full agreement with the direct two-loop PT generalization for the case where a mass-less quark-loop is present in the two-loop diagrams, which has been presented in S. Bauberger, F.A. Berends, M. Böhm, M. Buza and G. Weiglein, Nucl. Phys. Proc. Suppl. **B37**, 95 (1994).

[45] C. Becchi, A. Rouet, and R. Stora, Ann. Phys. (NY) **98**, 287 (1976).

[46] See, *e.g.*, T.-P. Cheng and L.-F. Li, *Gauge Theory of Elementary Particle Physics*, Clarendon Press, Oxford, 1985, p. 277.

[47] Yu.L. Dokshitzer, D.I. Dyakonov, and S.I. Troyan, Phys. Rep. **58**, 269 (1980); A. Andraši and J.C. Taylor, Nucl. Phys. **B192**, 283 (1981); D.M. Capper and G. Leibbrandt, Phys. Rev. **D25**, 1002 (1982).

[48] See, *e.g.*, third paper of [34].

[49] N.J. Watson, Phys. Lett. **B349**, 155 (1995).

[50] R.D.Pisarski, private communication.

[51] G. Grunberg, Phys. Rev. **D40**, 680 (1989); Phys. Rev. **D46**, 2228 (1992).

[52] R. Haussling, E. Kraus, K. Sibold, Nucl. Phys. **B539**, 691 (1999).

[53] The corresponding PT constant at one-loop was first presented in [30].

[54] I thank G. Grunberg and E. Gardi for emphasizing this point to me.

[55] P. Gambino and A. Sirlin, Phys. Lett. **B355**, 295 (1995).

[56] R. Kallosh, Nucl. Phys. **B78**, 293 (1974).

[57] T.Kinoshita, J. Math. Phys. **3**, 650 (1962); E.C.Poggio and H.R.Quinn, Phys. Rev. **D14**, 578 (1976); G.Sterman, Phys. Rev. **D14**, 2123 (1976).

[58] Taizo Muta, *Foundations of Quantum Chromodynamics*, World Scientific Lecture Notes in Physics –Vol.5, 1987, ch.6.

[59] S. Catani and E. D'Emilio, Fortsch. Phys. **41**, 261 (1993).

[60] Yu.L. Dokshitzer, G. Marchesini, and B.R. Webber, Nucl. Phys. **B469**, 93 (1996)

[61] F. Halzen, G. Krein and A.A. Natale, Phys. Rev. **D47**, 295 (1993); M.B. Gay Ducati, F. Halzen and A.A. Natale, Phys. Rev. **D48**, 2324 (1993); J.R. Cudell and B.U. Nguyen, Nucl. Phys. **B420**, 669 (1994); A. Donnachie and P.V. Landshoff, Phys. Lett. **B387**, 637 (1996); B.Magradze, hep-ph/9911456.

[62] Y.J. Feng, C.S. Lam, Phys.Rev. **D50**, 7430 (1994).

[63] Z. Bern and D.C. Dunbar, Nucl. Phys. **B379**, 562 (1992), and references therein.

[64] P. Di Vecchia, L. Magnea, A. Lerda, R. Russo, and R. Marotta, Nucl. Phys. **B469**, 235 (1996).

[65] P. Gambino and P.A. Grassi, *The Nielsen Identities of the SM and the Definition of Mass* hep-ph/9907254.

[66] C. Schubert, *An Introduction to the Worldline Technique for Quantum Field Theory Calculations*, Lectures given at 36th Cracow School of Theoretical Physics, Zakopane, Poland, 1-10 Jun 1996, Acta Phys. Polon. **B27**, 3965 (1996), and references therein.

[67] W. Beenakker, F.A. Berends, A.P. Chapovsky, *An Effective Lagrangian Approach for Unstable Particles* hep-ph/9909472.

Figure Captions

Fig.1: Carrying out the fundamental vertex decomposition inside the non-abelian Feynman graph contributing to $\Gamma_\alpha^{(2)}$ (a), gives rise to a genuine vertex (b) and a self-enery-like contribution (c).

Fig.2: The diagrammatic representation of PT one-loop self-energy $\widehat{\Pi}_{\alpha\beta}^{(1)}$, as the sum of the conventional self-energy $\Pi_{\alpha\beta}^{(1)}$, graphs (a) and (b), and the pinch contributions coming from the vertices (c).

Fig.3: The PT one-loop vertex $\widehat{\Gamma}_\alpha^{(1)}$.

Fig.4: The one-particle reducible graphs before $[(a), (b), (c), (d)]$ and after $[(e), (f), (g), (h)]$ the PT rearrangement. $G^{(1)}$ and $\widehat{G}^{(1)}$ denote respectively the conventional and PT one-loop vertices with one-loop self-energy corrections to the external fermions included.

Fig.5: The PT rearrangement of typical one-particle reducible graph (a), giving rise to its PT counterpart (a^P), and to contributions to the first term of $F_P^{(2)}$ (c) and to $Y_P^{(2)}$ (b).

Fig.6: The result of enforcing the PT decomposition on the external vertices of some of the two-loop Feynman diagrams contributing the conventional two-loop quark-gluon vertex $\Gamma_\alpha^{(2)}$.

Fig.7: The result of enforcing the PT decomposition on the external vertices of some of the remaining two-loop vertex graphs.

Fig.8: The Feynman diagrams contributing to the conventional two-loop gluon self-energy $\Pi_{\alpha\beta}^{(2)}$, in the R_ξ gauges.

Fig.9: The Feynman diagrams contributing to the BFM two-loop gluon self-energy $\widetilde{\Pi}_{\alpha\beta}^{(2)}$.

Fig.10: The one-loop counterterms contributing to the conventional two-loop gluon self-energy $\Pi_{\alpha\beta}^{(2)}$.

Fig.11: The one-loop counterterms necessary for the two-loop gluon self-energy $\widehat{\Pi}_{\alpha\beta}^{(2)}$; they are identical to those needed for the BFM two-loop gluon self-energy $\widetilde{\Pi}_{\alpha\beta}^{(2)}$.

Fig.12: The one-loop counterterms necessary to cancell the sub-divergences inside the conventional two-loop quark-gluon vertex $\Gamma_\alpha^{(2)}$. In the case of massive fermions the wave-function counterterm $K_2^{(1)}$ should be accompanied by the appropriate mass counterterm (not shown).

Fig.13: The one-loop counterterms necessary to cancell the sub-divergences inside the PT two-loop quark-gluon vertex $\widehat{\Gamma}_\alpha^{(2)}$; they are identical to those neede for the BFM two-loop quark-gluon vertex $\widetilde{\Gamma}_\alpha^{(2)}$.

Fig.14: The fundamental BRS-enforced cancellation of s-channel (a) and t-channel $[(d_1)$ and $(d_2)]$ contributions, instrumental for the absorptive PT construction. Graph (b) gives rise to the correct ghost-structure.

Fig.15: The Cutkosky cuts of the PT (and BFMFG) one-loop gluon self-energy.

Fig.16: The one-loop amplitude for the process $q(k_1)\bar{q}(k_2) \to g(p_1)g(p_2)$, after the PT rearrangement.

Fig.17: The Feynman diagrans contributing to the conventional one-loop three-gluon vertex $\Gamma_{\alpha\mu\nu}^{(1)}$.

Fig.18: The diagrammatic representation of the one-loop three-gluon vertex $\Gamma_{F\alpha\mu\nu}^{(1)}$.

Fig.19: Some of the one-loop t-channel graphs contributing to $q(k_1)\bar{q}(k_2) \rightarrow g(p_1)g(p_2)$.

Fig.20: The two-particle Cutkosky cuts of the PT (and BFMFG) two-loop gluon self-energy. We have used the same labelling of individual diagrams as in Fig. 9. The two upper (lower) rows show graphs where two gluon (ghost) lines have been cut.

Fig.21: The tree-level graphs contributing to the process $q(k_1)\bar{q}(k_2) \rightarrow g(p_1)g(p_2)g(p_3)$, after the PT rearrangement.

Fig.22: The three-particle Cutkosky cuts of the PT (and BFMFG) two-loop gluon self-energy. We have used the same labelling of individual diagrams as in Fig. 9. The first five graphs have three-gluon cuts, the next two have two-gluon-one-ghost cuts, while the remaining ones have one-gluon-two-ghost cuts.
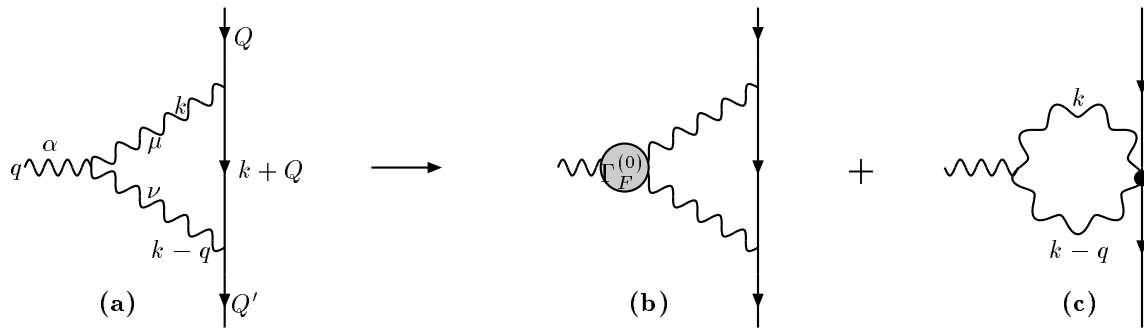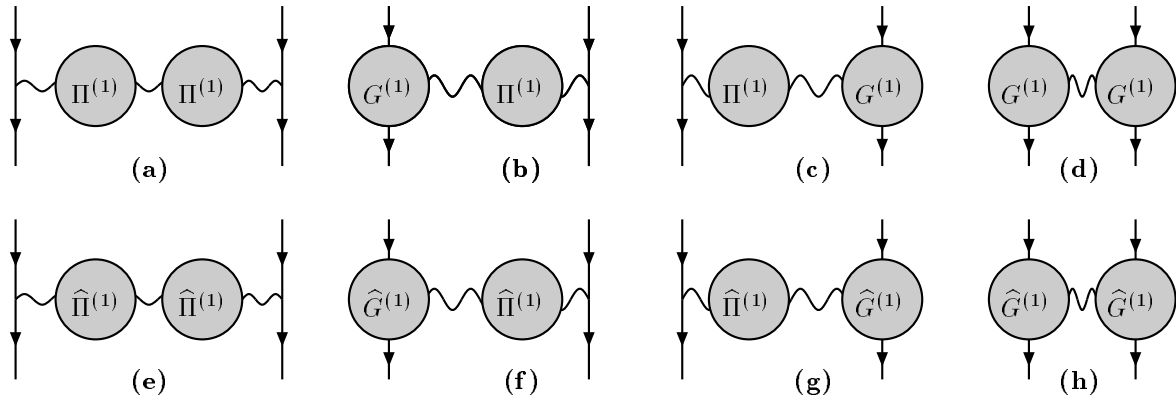
Fig. 1

Fig. 2

Fig. 3

Fig. 4

Fig. 5

Fig. 6

$(\mathbf{r_1})$ $(\mathbf{r_1^F})$ $(\mathbf{a})$

$(\mathbf{b})$ $(\mathbf{c})$

$(\mathbf{r_2})$ $(\mathbf{r_2^F})$ $(\mathbf{d})$ $(\mathbf{e})$ $(\mathbf{f})$

$(\mathbf{r_3})$ $(\mathbf{r_3^F})$ $(\mathbf{g})$ $(\mathbf{h})$

Fig. 7

(a)   **(b)**   **(c)**   **(d)**

(e)   **(f)**   **(g)**   **(h)**

(i)   **(j)**   **(k)**   **(ℓ)**

Fig. 8

(a)   **(b)**   **(c)**   **(d)**

(e)   **(f)**   **(g)**   **(h)**

(i)   **(j)**   **(k)**   **(ℓ)**

(m)   **(n)**   **(o)**   **(p)**

(q)   **(r)**   **(s)**

Fig. 9

(a)

(b)

(c)

(d)

(e)

(f)

(g)

Fig. 10

(a)

(b)

(c)

Fig. 11

Fig. 12

Fig. 13

(a)   (b)   (c)

(d)   (c)

Fig. 14

$$\Im m \widehat{\Pi}^{(1)}_{\alpha\beta}(q) \;=\; (\tfrac{1}{2})\, \widetilde{A}_\alpha \;\mathord{\sim\!\!\sim}\; \widetilde{A}_\beta \;+\; \widetilde{A}_\alpha \;\mathord{\sim\!\!\sim}\; \widetilde{A}_\beta$$

(a)   (b)

Fig. 15

$$\mathcal{T}_{\mu\nu} =$$

$\widehat{\Pi}^{(1)}_{\alpha\beta}$ $\Gamma^{(0)}_F$ q p_1 p_2 (a)

$\Gamma^{(1)}_F$ (b)

t-channel graphs (c)

$\Gamma^{(0)}_F$ $\Pi^{(1)}$ (e)

$\Pi^{(1)}$ $\Gamma^{(0)}_F$ (d)

Fig. 16

Fig. 17

Fig. 18

(a)   **(b)**   **(c)**

(d)   **(e)**   **(f)**   **(g)**

(h)   **(e)**   **(j)**   **(k)**

Fig. 19

$\widetilde{A}$ $\widetilde{A}$

(a)   (b)   (d)   (f)

(j)   (g)   (h)

(i)   (e)   (m)   (n)

(q)   (r)

Fig. 20

p_1, μ, a

k_1

$\Gamma_F^{(0)}$

p_2, ν, b

k_2

p_3, ρ, c

(a)

(b)

(c)

(d)

+ crossed

+ crossed

+ crossed

(e)

(f)

(g)

+ 5 permutations

(h)

Fig. 21

(a)   **(b)**   **(c)**   **(g)**

(ℓ)   **(e)**   **(f)**

(i)   **(j)**   **(k)**   **(h)**

(m)   **(n)**   **(o)**   **(p)**

(q)   **(r)**   **(s)**

Fig. 22